THESIS FOR THE DEGREE OF DOCTOR OF PHILOSOPHY

Novel approaches for achieving full density powder metallurgy steels

MAHESWARAN VATTUR SUNDARAM

Department of Industrial and Materials Science

CHALMERS UNIVERSITY OF TECHNOLOGY

Gothenburg, Sweden, 2019

Novel approaches for achieving full density powder metallurgy steels

MAHESWARAN VATTUR SUNDARAM

ISBN: 978-91-7597-881-9

Doktorsavhandlingar vid Chalmers tekniska högskola
Ny serie nr 4562
ISSN: 0346- 718X

Printed by Chalmers Reproservice
Gothenburg, Sweden 2019

Novel approaches for achieving full density powder metallurgy steels

Maheswaran Vattur Sundaram
Department of Industrial and Materials Science
Chalmers University of Technology

Abstract

Powder metallurgy (PM) is one of the most resource-efficient methods for manufacturing structural components with complex shapes. The utilisation of the metal powder to shape the components allows to minimise material waste and increase energy efficiency. However, with increased usage of PM parts in high-performance applications, there is a demand for components that can withstand extreme loading conditions with properties being equivalent or better than those of their wrought counterparts. The PM steel components fabricated through press and sinter route, even with all their advantages, have limitations due to the presence of residual porosity. Hence, it is desirable to reach full density to meet the highest performance demands. This study covers different powder consolidation approaches for water atomised steel powder with the aim of reaching near full density. This is achieved through the following processes: cold isostatic pressing (CIP) followed by sintering, liquid phase sintering (LPS), double pressing-double sintering (DPDS). These approaches were complimented by capsule free hot isostatic pressing (HIP) to reach full density.

Densification and subsequent enhancement of mechanical properties are to a certain extent directly connected to the successful removal of the surface oxide layer, covering the metal particles. This behaviour is especially critical in the case of powder pre-alloyed with oxygen-sensitive elements as chromium. The hydrogen in the sintering atmosphere reduces most of the surface iron oxide layer and any oxide residues are transformed into more stable oxides rich in Cr and Mn. Vacuum sintering provides oxide reduction through the formation of better local microclimate in the pores. When the powder is encapsulated and processed using HIP, the initial surface oxide is transformed into stable oxide particles that decorate the particle boundaries. Based on these results a model of oxide transformation during powder consolidation is proposed with regards to the alloy composition, powder properties and processing conditions.

In order to realise full density, CIP is utilised for consolidating iron powder and Cr-Mo pre-alloyed water atomised powder to reach a relative density of around 95% in sintered state to attain surface pore closure. This allows for subsequent HIP without capsule to reach full density. In case of Mo pre-alloyed powder, the LPS approach utilising Ni-Mn-B master alloy was established for enhanced sintering and densification. The best mechanical properties were then obtained with 0.12 wt.% of boron that allowed reaching as-sintered relative density of up to 96%. In addition, pore free surface was obtained after sintering that enabled capsule-free HIP to reach full density. Through the DPDS process, a pore free surface could also be achieved, which enabled reaching full-density through the subsequent HIP. Even though fine powder showed better densification, the density gradient in the compact persisted from the first pressing is there as the low-density region i.e., neutral zone, in the middle of the compact even after second pressing and HIP. Hence, optimisation during the first pressing is necessary to avoid this phenomenon.

All the above approaches represent different methods of achieving full density and selection of the appropriate method depends on the required geometry, alloy composition and hence resulting properties, number of components, cost, etc. Based on the analysis of the different methods it can be concluded that the combination of the tailored alloy concepts and consolidation techniques allows manufacturing of complex-shaped full-density PM components for high-performance applications.

Keywords: powder metallurgy steels, water atomised powder, Cr- and Mo-alloyed PM steels, sintering, vacuum sintering, high density, full density, master alloy, liquid phase sintering, cold isostatic pressing, double pressing-double sintering, hot isostatic pressing.

PREFACE

This PhD thesis is based on the work performed at the Department of Industrial and Material Science at Chalmers University of Technology under the supervision of Professor Eduard Hryha and Professor Lars Nyborg. This work has been performed within the framework of several projects supported by mainly VINNOVA and with correlation to a project supported by Swedish Foundation for Strategic Research.

The thesis will introduce the topic of powder metallurgy with further review of the high-density PM steels and its processes followed by chapters on various high-density approaches. The summary is based on the appended papers listed below:

I. Effect of density and processing conditions on oxide transformations and mechanical properties in Cr-Mo-alloyed PM steels
M. Vattur Sundaram, E. Hryha, D. Chasoglou, A. Rottstegge, L. Nyborg
In Manuscript

II. Vacuum sintering of chromium alloyed powder metallurgy steels
M. Vattur Sundaram, S. Karamchedu, C. Gouhier, O. Bergman, E. Hryha, L. Nyborg
Metal Powder Report (2019), Article in Press

III. XPS analysis of oxide transformation during sintering of chromium alloyed PM steels
M. Vattur Sundaram, E. Hryha, and L. Nyborg
Powder Metallurgy Progress, Vol. 14, (2014), no. 2, pp. 85–92

IV. Capsule-free hot isostatic pressing of sintered steel to full density using water atomized Fe and Cr-alloyed powder consolidated by cold isostatic pressing
M. Vattur Sundaram, E. Hryha, M. Ahlfors, O. Bergman, S. Berg, L. Nyborg
In Manuscript

V. Enhanced densification of PM steels by liquid phase sintering with boron containing master alloy
M. Vattur Sundaram, K.B. Surreddi, E. Hryha, A. Veiga, S. Berg, F. Castro, L. Nyborg
Metallurgical and Materials Transactions A, Vol 49, (2018), no.1, pp. 255-263

VI. Full densification in PM steels through liquid phase sintering and HIP approach
M. Vattur Sundaram, K.B. Surreddi, E. Hryha, A. Veiga, S. Berg, F. Castro, L. Nyborg
Proceedings of EuroPM 2018, Bilbao, Spain, (2018)

VII. Experimental and finite element simulation study of capsule-free hot isostatic pressing of sintered gears
M. Vattur Sundaram, A.Khodaee, M. Andersson, L. Nyborg, A. Melander
The International Journal of Advanced Manufacturing Technology, Vol 99, (2018), no.5-8, pp. 1725-1733

Contribution to the appended Papers

I. The author took part in planning with the co-authors and performed the experimental work and wrote the paper with the cooperation of the co-authors.

II. The author was involved in the planning and engaged in experiments together with co-authors. The author wrote the paper in co-operation with the co-authors.

III. The author planned and performed the experimental work in cooperation with the co-authors and also wrote the paper in collaboration with the co-authors.

IV. The author planned and performed the experimental work with co-operation of the co-authors and also wrote the paper.

V. The author planned and performed the experimental work in collaboration with the co-authors and wrote the paper with the cooperation of co-authors.

VI. The author planned and performed the experimental work in collaboration with the co-authors and wrote the paper with the cooperation of co-authors.

VII. The author planned and performed the experimental work and wrote the paper with the cooperation of co-authors. The co-author from KTH performed the FEM simulations.

Papers other than the appended

i. **Hot isostatic pressing of the water atomized steel powder: possibilities and challenges**
E. Hryha, M. Vattur Sundaram, A. Weddling, M. Bram, D. Chasoglou, L. Nyborg, W. Theisen
Proceedings of WORLD PM 2018, Beijing, China 2018

ii. **Approaches to reach fully dense powder metallurgical materials**
M. Vattur Sundaram, E. Hryha, and L. Nyborg
Proceedings of WORLD PM 2018, Beijing, China 2018

iii. **Manufacturing of valve bridge component utilizing lean alloyed powders and vacuum sintering**
R. Shvab, M. Vattur Sundaram, D. Chasoglou, H. Karlsson, S. Berg, E. Hryha, L. Nyborg
Powder Metallurgy Progress, vol. 18, no. 1, pp. 31–39, 2018.

iv. **Effect of alloying type and lean sintering atmosphere on the performance of PM components**
M. Vattur Sundaram, R. Shvab, Sten Millot, E. Hryha, L. Nyborg
Powder Metallurgy Progress, vol. 17, no. 2, pp. 72–81, 2017.

v. **Vacuum sintering studies on chromium alloyed PM steels**
M. Vattur Sundaram, S. Karamchedu, C. Gouhier, E. Hryha, L. Nyborg
Proceedings of World PM 2016, Germany 2016

vi. **Reaching full density of 100Cr6 PM steel by capsule free hot isostatic pressing of high-velocity compacted material**
H. Magnusson, K. Frisk, M. Vattur Sundaram, E. Hryha, C. Åslund, B.-O. Bengtsson, M. Ahlfors, and S. Wiberg
Proceedings of World PM 2016, Hamburg, Germany 2016

vii. **Innovative powder based manufacturing of high performance gears**
A.Khodaee, M. Vattur Sundaram, M. Andersson, A. Melander, A. Strondl, I. Heikkilä, A. Miedzinski, L. Nyborg, and M. Ahlfors
Proceedings of World PM 2016, Hamburg, Germany 2016

viii. **As-HIP microstructure of EBM fabricated shell components**
A. Leicht, M. Vattur Sundaram, Y. Yao, E. Hryha, L. Nyborg, L.-E. Rännar, A. Koptioug, K. Frisk, and M. Ahlfors
Proceedings of World PM 2016, Hamburg, Germany 2016

CONTENTS

1 INTRODUCTION

1.1 Background

Powder metallurgy (PM) as a manufacturing technology has progressed rapidly during the last century, with structural PM parts constituting a significant portion of the PM components produced globally [1]. In Europe as of 2017, ferrous PM accounts for the 80% of the PM parts produced by volume and the automotive sector continues to be the major consumer [2]. The main advantage of PM lies in its low energy consumption and the ability to form complex shaped parts in high volumes with low material wastage. In addition, 80% of the raw material used for manufacturing of water atomised powder is from the recycled scrap, which makes PM even more resource efficient and overall sustainable manufacturing process [3], [4].

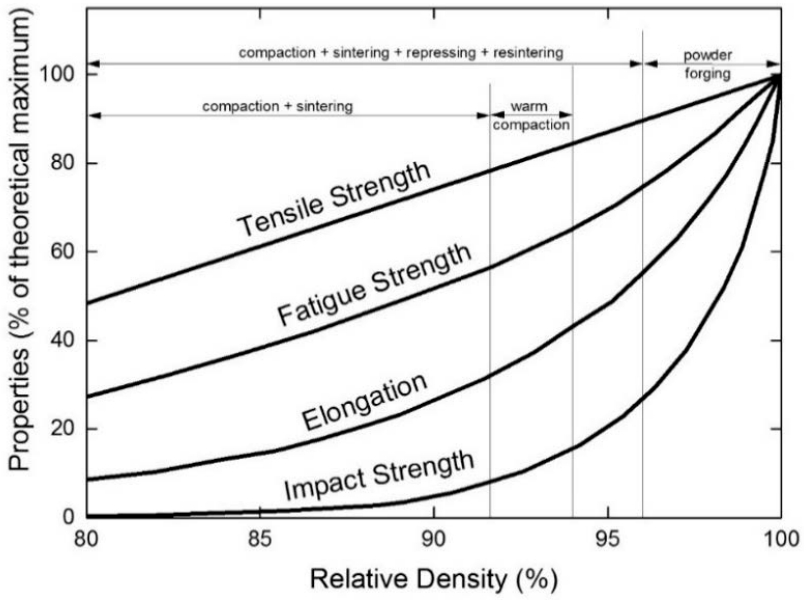

Figure 1: Mechanical properties vs the relative density of PM steels achieved by means of different processes, redrawn from [5].

The typical density of the structural PM steels manufactured from water atomised powder is between 7.0 to 7.2 g/cm^3, which is about 92% of the theoretical density and hence means around 8% of residual porosity. Pores, thus being the inherent feature in PM steels, will adversely affect the properties, limiting its potential for high-performance applications. Therefore, increasing the relative density is a key to overcome the challenge, especially for high-performance applications (such as gears, transmission parts and engine components) where the parts require to endure heavy loading conditions. Hence, there is a persistent drive towards improved densification to enhance the resulting properties. Figure 1 summarises the effect of density on the mechanical properties, showing a significant increase with relative density. It also highlights the role of typical PM processes in realising different density levels.

1.2 Densification approaches

Consolidation of metal powder to a final compact can be classified as a pressure-based, sintering-based and hybrid-based approaches [6]. Figure 2 summarizes the different methods connected to each approach. In order to achieve the intended densification, several approaches

can be utilised [7], [8]. All the listed approaches and processes in Figure 2 have their unique advantages and limitations. It is therefore essential to select the suitable process route for reaching full density according to the requirements of the specific application [3].

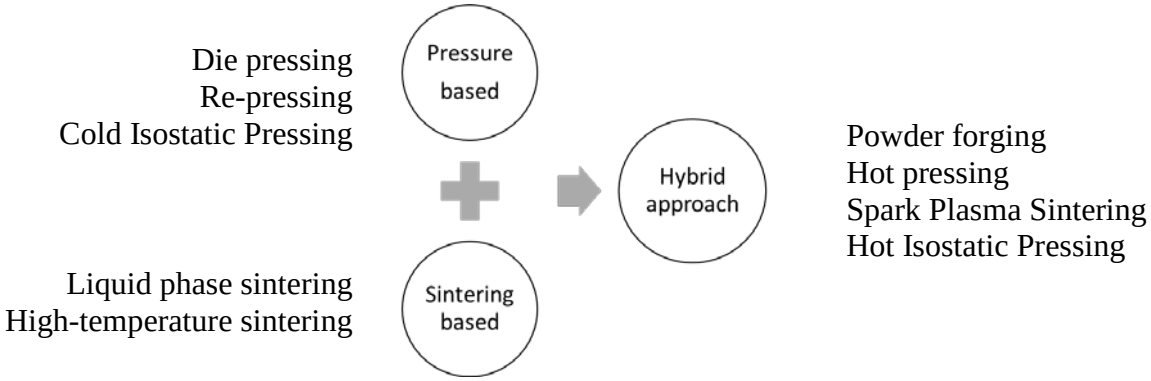

Figure 2: Different approaches for densification according to German [6].

To further assist in the process selection, Figure 3 maps the position of various technologies utilising metal powder in terms of mass range and economic batch size for manufacturing PM components. Processes such as press and sinter (P&S), powder forging (PF), and metal injection moulding (MIM) are suitable for high volume production. The P&S route is the most commonly used consolidation route and enables to form complex shaped components starting from a single pressing operation in high volumes. The PF allows full densification of parts with simple geometry, whereas MIM is the most suitable technology for manufacturing small-sized and complex-shaped components. In the case of PF there is usually prior P&S to set the preform for the forging step and MIM necessitates a final sintering stage to bring the material to required density.

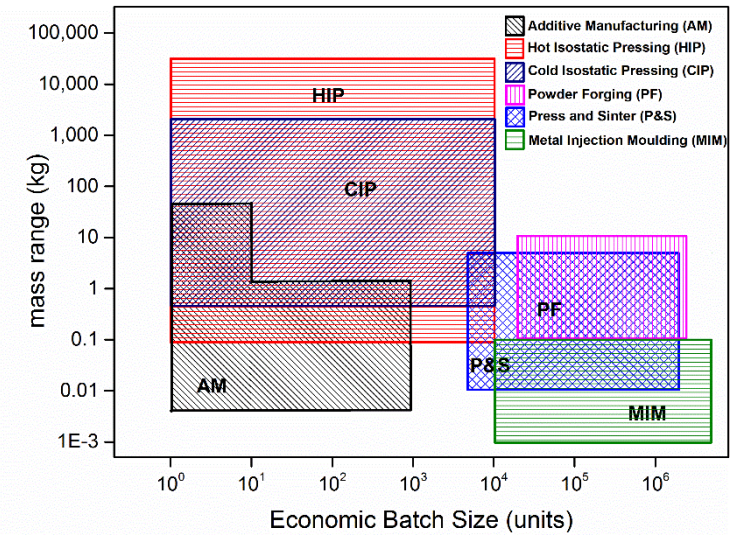

Figure 3: Position of various powder metal technologies based on the summary of data extracted from CES EduPack 2018 software [9], and other sources [1], [10], [11].

Additive manufacturing (AM), as a layer by layer approach, enfolds several technologies within its spectrum with the possibilities to manufacture a wide range of components in varying size and volume. Powder-based AM technologies represent a rapidly growing sector of powder

metallurgy, where powder bed fusion (PBF) (Laser-PBF and Electron beam-PBF), binder jetting (BJ) and direct energy deposition (DED) are the dominant ones. All these AM technologies allow for manufacturing complex shaped design which is otherwise not conceivable by traditional processing. They also typically cover low-size range and rather low manufacturing rate of the complex component in comparison to P&S and MIM, see Figure 3. Both isostatic processes, i.e., cold isostatic pressing (CIP) and hot isostatic pressing (HIP), are suitable for consolidating large-sized parts in a medium to small production rates. However, only simple geometries can be consolidated through CIP, whereas complex shapes can be attained through HIP. Note, however, that HIP is a single stage process in which the material is fully consolidated to full density from powder, while CIP is a shaping process like die pressing, which hence requires subsequent sintering or hot forming. The HIP as a post-processing operation is becoming widely accepted for MIM and AM components due to its benefit in removing the internal pores and defects, despite added cost. However, recent development in HIP technology has demonstrated that significant cost reduction is possible by integrating final heat treatment in the HIP process [12], [13].

For the metal powder industry to remain competitive and progress continuously, it is important to have an advantage over other manufacturing processes such as casting, forging, and machining. Moreover, enhanced density levels will open up a wide range of new applications for PM steels where improved properties are required. This pushes the limits of the existing processing conditions at the different stages.

1.3 Aim and scope of the thesis

The aim is to demonstrate how to achieve full density in PM steels by exploring various processes for selected materials. The scope of the thesis is hence divided into two parts: the development of processes and the tuning of materials for the selected processes.

1.3.1 Processes

The PM technologies utilised in this study, see Figure 4, which allows enhanced densification through existing processes, namely conventional die pressing followed by sintering, double pressing-double sintering (DPDS), cold isostatic pressing (CIP) followed by solid state sintering and liquid phase sintering (LPS). These processes enable to reach density levels ≥95% after sintering, which ensures surface pore closure [14] and allows for full densification by subsequent capsule free hot isostatic pressing (HIP) [15]–[17].

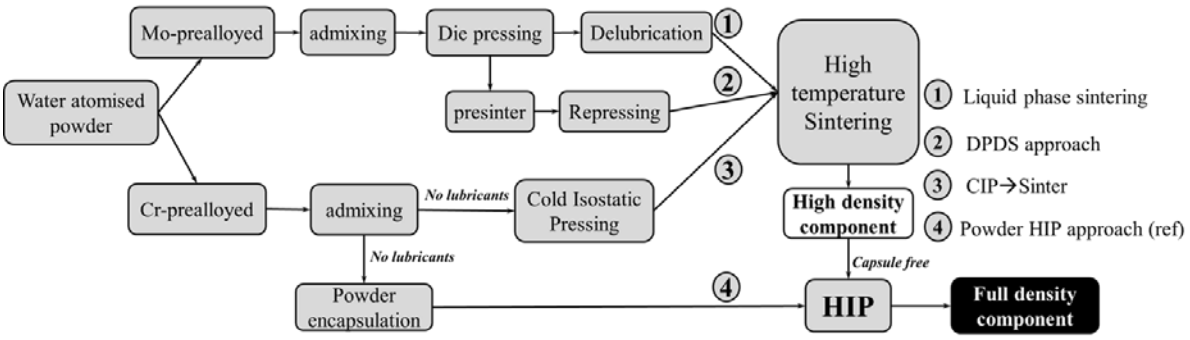

Figure 4: Process flow adopted in this study for full density consolidation.

From the process perspective, the main scope is thus *to critically evaluate the various approaches to reach full density as well as to develop new hybrid routes based on the state-of-the-art of the technologies applied.*

1.3.2 **Materials**

In terms of the material investigated, the model materials used are the existing high-performance alloys from the low alloy steel segment, namely PM steels pre-alloyed with Cr and Mo.

1.3.2.1 PM steels pre-alloyed with Cr

The PM steels pre-alloyed with Cr constitute a low-cost alternative with excellent sinter hardenability, though introduced two decades ago [18], yet poses challenges during both, compaction and sintering, owing to the affinity of Cr to form stable oxides. Hence, the critical aspect is to effectively reduce such oxides on the powder surfaces during the sintering and to enable the formation and growth of inter-particle necks, to create good inter-particle strength and ultimately also promote the achievement of higher sintered density. Even though the processing aspects are already addressed through several studies [19]–[23], it is still relevant for the current study as it is considered to be the benchmark of alloys owing to the oxygen sensitivity of Cr. The following research questions were framed from a scientific perspective to address the challenges involved in sintering high-density Cr-alloyed PM steels as given below:

- *What is the effect of density and processing conditions on the development and strength of the inter-particle necks?*
- *What are the oxide transformation mechanisms involved during different consolidation processes?*
- *What consolidation route can be used to fully densify this type of material to the near-net-shape components?*

1.3.2.2 PM steels pre-alloyed with Mo

PM steels pre-alloyed with Mo are characterised by good compressibility and low sensitivity to oxygen uptake. Hence, the focus for this alloy grades was placed on two approaches to reach higher sintered density: liquid phase sintering (LPS) and double pressing-double sintering (DPDS).

The presence of Mo in the base powder together with the boron is supposed to enhance the sintered density and properties owing to the liquid generation. In this study, the LPS approach is based on utilisation of boron-containing master alloy studied in collaboration with CEIT, Spain. The master-alloy was originally developed by CEIT [24], [25]. The aim of LPS in the case in question was not only to provide enhanced density but also to have an excellent dimensional control of the PM steel during the sintering. This is provided by the master-alloy system used thanks to the ability to form a surface-densified layer. Hence, the research question framed for this system was:

- *What is the role of boron-containing master alloy on the densification and how does it affect the process window?*

The DPDS approach was initiated by Höganäs AB [26] with the aim to achieve high enough density level. Water atomised steel powder pre-alloyed with Mo is known for its excellent compressibility and the sintered material is typically used for case hardening applications. The good compressibility makes the Mo-alloyed grades ideal materials for the DPDS approach and the following research question was therefore phrased:

- *How to reach near-full density PM steel components with complex geometry through the tailored powder and DPDS process route?*

2 THE POWDER METALLURGY PROCESS

Powder metallurgy (PM) as an industrial process has grown rapidly within the last century, beginning with the development of cemented carbides, self-lubricating bearings and moving on to the structural ferrous parts [27]. The current focus is towards developing PM steels for high-performance applications.

Figure 5: Typical PM steel process flow considering press and sinter route.

The PM process through press and sinter route is considered to be the most energy and material efficient technology for fabrication of the complex-shaped structural components in comparison to conventional processes such as casting, forging and machining [28], [29]. The other advantages are flexibility in alloy design and compositional control which are not possible by other methods. The typical PM steel process involves various stages, as seen in Figure 5. It begins with the powder production, followed by further alloying, compaction, sintering and post-processing. Each stage requires strict process control, starting from producing high-quality powder, the addition of further alloying elements and choosing an alloying method, effective lubricants and pressing method, control of sintering and the final required post-sintering operations.

2.1 Powder production

Atomisation is the most common method for producing metal powder. During atomisation, a stream of molten metal is disintegrated by high-pressure water or inert gas injected through the nozzles at a high velocity. The liquid metal will disintegrate into fine droplets and solidify into metal particles with the shape and microstructure determined by the atomising medium and cooling rate.

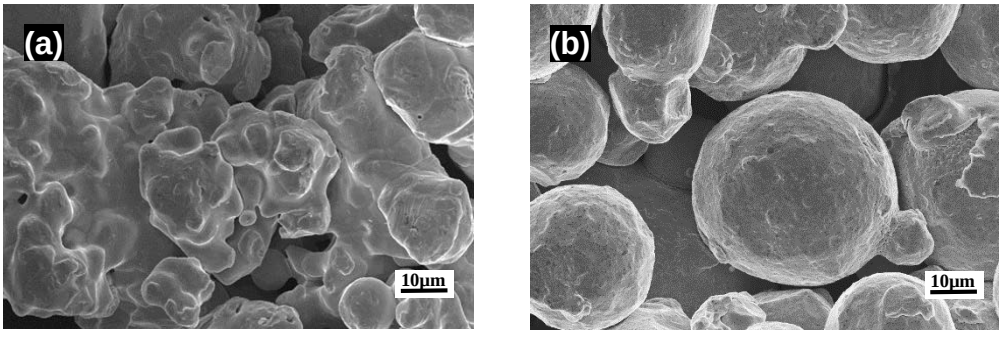

Figure 6: SEM micrographs showing typical powder morphology of water (a) and gas (b) atomised powder.

Water atomisation is used in case of low alloyed steel powder and gas atomisation is commonly used for manufacturing powder that is sensitive to oxidation such as high-alloyed steels, stainless steels, tool steels, superalloys, titanium and its alloys, etc.

The powder morphology differs between the two methods in the sense that irregular and spherical shaped particles are obtained when water and gas are used, respectively. The characteristics of water atomised powder, see Figure 6 (a), being irregular in shape, is suitable for compaction since this shape helps in the better interlocking of the metal particles during and after pressing. This in fact contributes to the green strength of the part. Gas atomised powder has typically spherical shape, as shown in Figure 6 (b). Such powder therefore exhibits good flowability but cannot be compacted by means of uniaxial pressing. Water atomised powder is covered by a thicker oxide layer after atomisation and hence is subsequently annealed in reducing atmosphere after atomisation to remove oxides and to obtain good compressibility. After the annealing, the powder surface is covered by a thin oxide layer of the base metal with the presence of only low amount of oxide particulates. The thin oxide layer is ultimately the result of the powder handling in the air after annealing, while the stable oxide particulates being the remains from the annealing. Depending on the alloying elements present, the particulate surface features will have higher content of strong oxide formers accordingly. In the case of the gas atomised powder, an additional annealing procedure is not required as the powder possesses high purity after atomisation. It should be noted that for high alloy steel like stainless steel, there is no need for annealing of water atomised powder.

2.2 Alloying

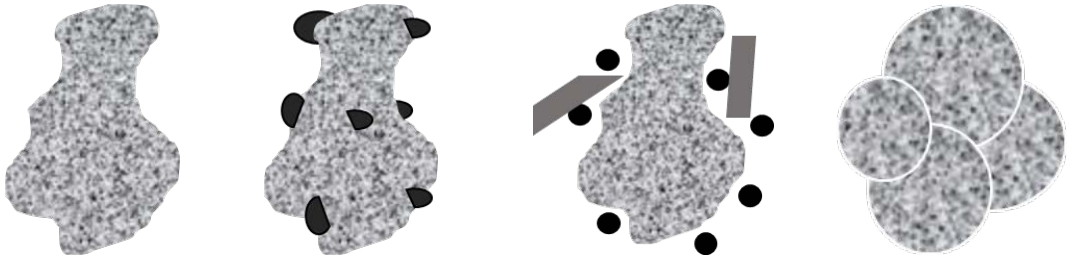

Figure 7: Schematic illustration of differently alloyed powder (a) pre-alloyed (b) diffusion bonded (c) admixed and (d) agglomerated powder.

*2.2.1 **Pre-alloying***

In the case of pre-alloying, the alloying elements are added to the molten metal during atomisation. This applies especially for elements like Cr, Mn etc., which have a greater affinity towards oxygen. For water atomised powder it is essential that the elements should provide limited solid solution strengthening so that compressibility is not affected. Pre-alloying enables the homogenous distribution of the alloying elements as indicated in Figure 7 (a), which results in dimensional stability after sintering.

2.2.2 ***Diffusion bonding***

Pure iron or pre-alloyed powder is mixed with a fine elemental powder of e.g. Ni, Cu, etc., and the mixture is heat-treated in a reducing atmosphere. The fine powder of alloying elements will bond to the base iron particles through diffusion, see Figure 7 (b).

2.2.3 ***Admixing***

This is a flexible method of producing powder mixes by mixing iron/steel powder with the powder of required alloying elements. Generally, graphite, additives and lubricants are mixed in this way, see Figure 7 (c).

2.2.4 ***Powder agglomeration***

The gas atomised powder is agglomerated using a binder to form agglomerates that look like irregularly shaped particles, as in Figure 7 (d), providing consolidation opportunity and green strength after pressing [30].

2.3 Compaction

Uniaxial compaction or die pressing is the most common method of consolidation in PM steels. Water atomised powder admixed with lubricant and graphite is filled in the die cavity and pressed by the axial movement of the punches [31]. The compaction pressure is typically between 400 to 1000 MPa. During the powder pressing, the metal particles will rearrange with the pressure exerted by the punches and interlocking occurs due to their irregular shape. Sometimes even cold welding of the particles can take place at high pressures. This gives the compacts sufficient green strength for further handling. After pressing there is a density gradient due to the differences in pressure distribution because of the moving punches and solid die. This density gradient is formed in the surface region along the compaction direction owing to the frictional resistance at die wall, while it is much less pronounced inside the compact.

The typical compaction presses are either mechanical or hydraulic type with the multilevel punch movements. For the multilevel components (e.g. synchroniser hubs and oil pump gears) to have an uniform densification and to avoid variation in density among different sections, the punches move relative to one another with the help of platens according to the density requirements of different sections in the component [31]. The component size is limited by its weight and the aspect ratio (height to diameter ratio) since the ejection forces will be too high with the increased height, generating more friction. The final properties and dimensions of the obtained PM component depend heavily on the compaction. Other possible ways to overcome these issues and have high density after pressing [32]–[34] are addressed in Chapter 3.

2.4 Delubrication

The additives, such as lubricants or binders, admixed before the compaction step must be removed entirely before sintering. In the case of the gaseous sintering process, delubrication is carried out in the zone before the sintering zone in a continuous sintering furnace. The typical temperature recommended for the delubrication of Cr-alloyed PM steels is 450 °C for 30 minutes in a dry inert (e.g. nitrogen) atmosphere [23]. At this temperature, the powder characteristics remain unchanged after delubrication. The removal of the lubricant occurs in two stages: melting, and decomposition [23]. The parameters affecting delubrication are initial

density, heating rates, sample geometry, gas flow rate, temperature, and processing gas composition. Improper control of these parameters can adversely affect the final properties of the components after subsequent sintering.

2.5 Sintering

Sintering imparts necessary strength to the component by creating bonding between the metal particles. Sintering is usually performed below the melting point at roughly 75-80% of the melting temperature. A typical powder particle will tend to have a larger specific surface area as compared to a solid material which contributes to the increased surface energy. The main driving force for sintering is to minimise the excess free energy by reducing the specific surface area, which is dominant for fine powders. In the case of solid-state sintering of PM steels utilising coarser powders, surface diffusion is dominant for the atoms to migrate through point of contact by forming inter-particle necks. Besides, the densification will happens only through the bulk transport of the atoms not through the surface diffusion of atoms. The inter-particle necks once formed are developed by the mass transport between the adjoining metal particles. The degree of sintering is determined by the number and strength of the established sinter necks.

In addition, the formation and growth of inter-particle necks are enabled by early and efficient reduction of the surface oxides covering the powder particles [35], [36]. Sintering in reducing atmospheres removes the surface oxides. Admixed graphite also plays a vital part by reducing the oxides through direct and indirect carbothermal reduction mechanisms, especially during vacuum sintering, where the carbon is the primary reducing agent involved in the removal of the oxides. The following reactions takes place during sintering of water atomised PM steels:

- Dissociation of oxides: $\frac{2}{y}Me_xO_y = \frac{2x}{y}Me + O_2$ (1)
- Reduction by hydrogen (400 – 550°C): $\frac{2}{y}Me_xO_y + 2H_2 \rightarrow \frac{2x}{y}Me + 2H_2O$ (2)
- Direct carbothermal reaction (~720°C): $Me_xO_y + yC \rightarrow xMe + yCO$ (3)
- Indirect carbothermal reaction (>900°C): $Me_xO_y + yCO \rightarrow xMe + yCO_2$ (4)
- Boudouard's Equilibrium (~720 °C) $C + CO_2 \rightleftharpoons 2CO$ (5)

In PM steels, endo-gas is the most commonly used sintering atmosphere as it provides necessary oxide reduction in case of easily-reducible iron oxide, followed by carbon restoration during cooling. When it comes to Cr-alloyed PM steels, hydrogen-containing atmospheres, typically N_2-10%H_2, are used as a processing atmosphere to assure efficient oxide reduction. Hence, the particular focus during sintering in nitrogen/hydrogen mixes should be placed on carbon control during sintering as it is vital to reach the required properties [37]. Studies on lean sintering atmospheres containing carbon monoxide have shown that the CO acts as both, reducing-oxidising and carburising-decarburising agent [23]. This implies that the proper control of the atmosphere during sintering is critical for the robust PM steel processing and tailoring the required sintered properties. Apart from the solid state sintering, which mainly contributes to the strengthening of PM steel, liquid phase sintering (LPS) can be applied to improve densification without changing the requirements on compaction stage and hence minimising

demands on new equipment solutions for compaction. A section on LPS is given in detail in the Chapter 3.

2.6 Secondary Operations

Following the sintering, the secondary operations involved very much depend on the part specific requirements that it has to fulfil. There are some operations, such as sizing or repressing, aiming to increase the density and retain the final dimensional tolerances. Heat treatments such as steam treatment, case hardening (carburising, nitriding, induction hardening, etc.) are performed to obtain the desired microstructure. Heat treatment processes are usually followed by tempering. Continuous sintering process offers another advantage of rapid cooling in the cooling zone after sintering with a cooling rate of ~ 2.5 to 5 °C/s, which allows for the component hardening. This is called sinter hardening as it combines sintering and hardening in a single process [38]. As mentioned above, all the secondary hardening processes can be avoided by sinter hardening. Tempering at 200 or 300 °C is performed to improve the toughness of the components, involving relieving the stresses induced during the hardening and the initial tempering of the martensitic microstructure. Optimised tempering temperature has shown to be important to avoid the dimensional instability associated with the PM steel components when utilised in an actual application [39], [40]. Depending on the requirements, other processes such as oil impregnation, machining, grinding, honing and lapping, can be applied as well.

3 FULL AND NEAR FULL DENSITY CONSOLIDATION PROCESSES

For the continuous progress of the PM industry, the trend towards reaching higher relative density levels should be emphasised. In order to reach full density, the combination of pressure and temperature is basically necessary. Applying only compaction or sintering alone would not be feasible. The high-density processing approaches involved are as follows:

- Warm compaction
- Warm die compaction
- Double pressing and double sintering (DPDS)
- Cold isostatic pressing (CIP)
- High-velocity compaction (HVC)
- Powder forging (PF)
- Liquid phase sintering (LPS)
- Hot pressing (HP)
- Spark plasma sintering (SPS)
- Additive manufacturing (AM)
- Hot isostatic pressing (HIP)

Reaching high or full density in PM steels is usually associated with high costs as compared to the conventional die pressing. For example, the relative cost of producing a component through powder forging to reach full density is about 200% of the conventional die pressing [41]. In order to achieve increased densification, several approaches can be utilised, either as a standalone process or by combining several approaches [7], [8]. All the above-listed processes have their unique advantages and limitations and therefore it is essential to select the suitable process route for reaching a full density according to the specific application and its requirement [3].

3.1 Warm compaction

In this process, both the die and powder are preheated to a temperature of 130 – 150° C at which compaction is performed [42], and the density is increased by 0.1 to 0.25 g/cm^3 compared to the cold die pressing [43]. Heating the powder to 150 °C from 25 °C slightly enables to reduce the compressive yield strength [44] and along with the optimised lubricant addition can provide a significant increase in density. This also allows for lower compaction pressures as compared to the cold die compaction.

3.2 Warm die compaction

Unlike warm compaction, only the die is now heated, and the powder remains at room temperature. This procedure allows for an increase in productivity and a decrease in process costs. However, lower density levels are achieved in comparison with the warm compaction, and the typical part size is limited to less than 1 kg [42]. High-density levels of 7.45 g/cm^3 can be reached by controlling the lubricant addition below 0.4 wt.% [45].

3.3 Double pressing-double sintering

In this process, the component is pre-sintered after the first pressing, which aids in lubricant removal and material annealing. This helps in further densification during the second pressing stage. The component is pressed once again and sintered at high temperature to reach higher density. The pores remaining after removal of the lubricant will be eliminated to some extent during this process, which enhances the density by 3 to 4%. This enables to avoid the distortions and retain the required tolerances and dimensions after second sintering. This approach can be considered as a hybrid temperature/pressure-based densification process. Sintering at high temperature is performed after second pressing to fully develop the inter-particle necks and thus enhance the density.

3.4 Cold isostatic pressing

In this process, uniform pressure is applied at room temperature through pressurising media like liquid or gas. It could be a wet bag or a dry bag process, depending on the moulds. In the wet bag process, a flexible rubber mould is filled with powder which is then sealed and evacuated. The mould with the powder inside is further placed directly in the cold isostatic pressing (CIP) chamber and exposed to the pressurising liquid. In the dry bag process, the flexible mould is fixed within the chamber and is filled with powder before each compaction cycle. The CIP is beneficial for consolidating large components by utilising flexible moulds at a lower cost; it also enables homogeneous density distribution without the need for lubricants. These features make CIP an attractive consolidation process [46] and reduce the distortions during sintering [3].

3.5 High velocity compaction

High velocity compaction (HVC) is suitable for reaching full densification and is up to 1000 times faster than the conventional pressing. In this process, powder densification is achieved through the intense shock waves generated by striking at high velocity. This high energy can be utilised to impact the samples once or twice based on the machine capacity. The components are characterised by uniform density with lower ejection force and spring back [47]. However, this process allows compaction of only simple geometries. The amount of lubricant can be reduced or even eliminated in some cases [48].

3.6 Powder forging

In this process, the compact either in green, pre-sintered or sintered state is hot forged into a final fully dense component [49]. The temperature at which the preform is heated in the case of ferrous material can be up to a maximum of 1200 °C [6]. Nearly all the automotive connecting rods, produced nowadays, are processed through powder forging to 100% density. The high productivity of 300 to 900 components per hour weighing between 0.1 to 5 kg can be achieved in powder forging [1].

3.7 Liquid phase sintering

Liquid phase sintered components account for ~70% of all the sintered goods in terms of cost, which includes high-speed steels, tool steels and especially hard metals [50]. Liquid phase sintering (LPS) is hence a well-known method to achieve densification through the addition of

low melting alloys or elemental powder that melts below the sintering temperature. Hence, the densification is assisted by liquid phase formation.

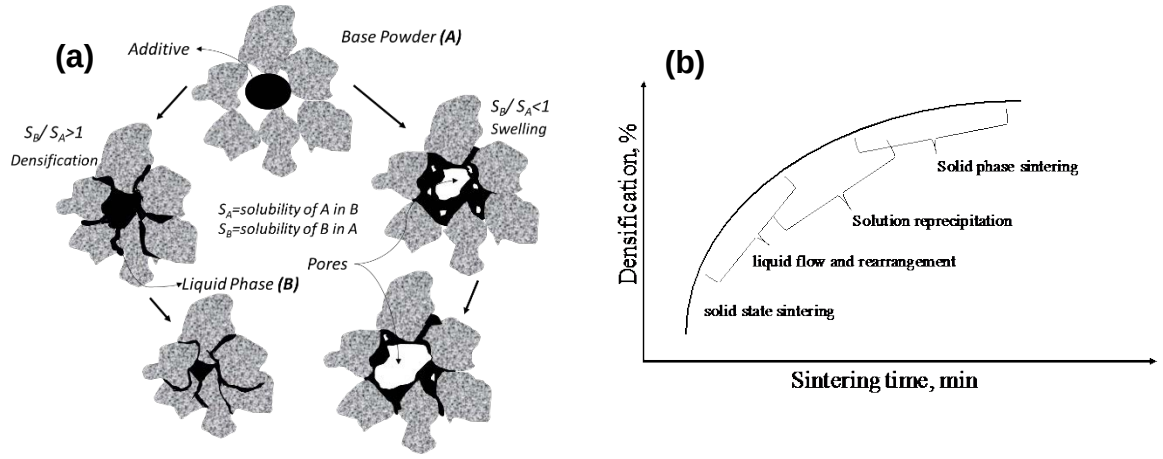

Figure 8: Densification and swelling associated with relative solubility of solid and liquid (a) redrawn from [51]*, and stages during liquid phase sintering (b) redrawn from* [52].

The LPS is employed mainly in the case of high-speed steels, tool steels and hard metals, for which the liquid phase formation is utilised for densification to its full potential. However, it is not a common approach for low alloy ferrous PM steel components. For ferrous PM, the liquid phase formers are added either in the form of elemental mix or as a master alloy. After the liquid generation, the compact either shrinks or expands, as can be seen in Figure 8 (a), according to the solubility of the base material in the liquid or the liquid in the base material. Hence, the solid solubility in liquid promotes densification, whereas the liquid solubility in solid results in swelling. Both mechanisms are dependent on the particle size, initial green density and sintering temperature. The initial powder size has a significant effect on the particles rearrangement during sintering. The irregular particles during the initial rearrangement will shrink rapidly as the contact between the particles is not perfect, and the liquid starts to fill the pores [52].

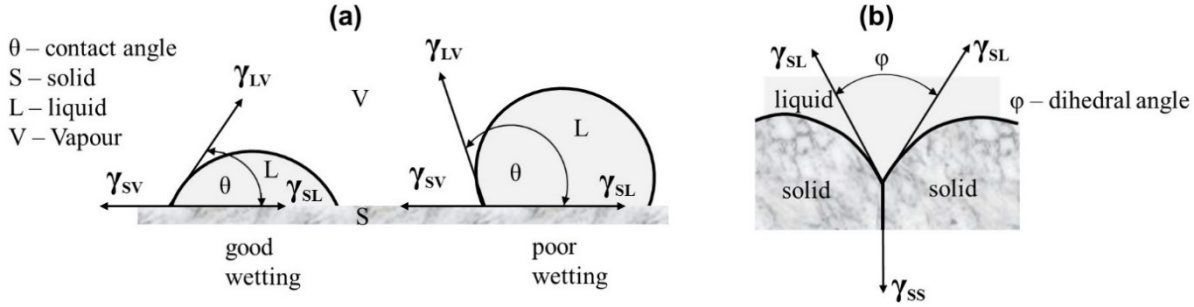

Figure 9: Wetting characteristics of the liquid on the solid surface showing the contact angle (a), and dihedral angle between solid-liquid interface with equilibrium surface energies (b) redrawn from [51].

The liquid phase sintering occurs in three stages after solid state sintering, through the initial particle rearrangement, intermediate solution-repreciptation and the final stage is through solid phase sintering, as shown in Figure 8 (b). During the LPS, the liquid once melted will spread

around the base metal particles as well as along the grain boundaries due to capillary forces which aids in the primary particle rearrangement that takes place in two stages: primary and secondary rearrangement. Having lower contact angle increases the liquid spreading due to the better wettability of the liquid resulting in densification. Whereas higher contact angle specifies poor wettability, resulting in swelling due to retreat of the liquid from the solid. Even addition of certain alloying elements will influence the wetting characteristics by altering the contact angle [53]. The relationship between the interfacial energy and the contact angle is illustrated in Figure 9 (a) and can be described by the equation (6):

$$\gamma_{SV} = \gamma_{SL} + \gamma_{LV} \cos\theta \qquad -(6)$$

The secondary rearrangement involves liquid penetration and clustering of powder particles, which is controlled by the dihedral angle formed along the grain boundary where it intersect the liquid, see Figure 9 (b). The liquid penetration in the grain boundary occurs when the dihedral angle approaches 0° by separating the grains, due to the relatively high ratio between the solid-solid and solid-liquid surface energy [51]. The relationship between the surface energy of the solid-solid and solid-liquid with the dihedral angle is indicated in Figure 9 (b) and given by equation (7):

$$\gamma_{SS} = 2\gamma_{SL} \cos\left(\frac{\varphi}{2}\right) \qquad -(7)$$

In LPS, smaller the contact angle and dihedral angle are, the better is the resulting densification. The dihedral angle tends to change during sintering until its attains equilibrium with the interfacial energy after the interfacial reactions are completed [51]. After initial rearrangement, the solution-repreciptation takes place with the following three phenomena: grain growth, grain shape accommodation and densification. All these processes occur simultaneously. The densification during this stage is mainly due to the pore filling by the liquid. The final stage of sintering pertains to pore elimination, grain coarsening and strengthening of the inter-particle necks without significant densification. During this stage, pores are isolated and the densification is driven by the pore filling mechanism but at a much slower rate than the intermediate stage. These pores are fragmented as a result of entrapped gases which can be inert or soluble in the matrix. Full densification is possible provided the gas can diffuse through or is soluble in the matrix, otherwise it will impede the densification [51].

The major concern for the LPS sintered components is to have a controlled shrinkage in order to have predictable dimensions after sintering for mass production. The distortions are uncontrolled changes in dimensions which alters the shape and cannot be controlled during the sintering. The green density of the compact, the volume fraction of liquid in the system, and the liquid viscosity are the parameters known to influence the shrinkage. Having too much liquid volume fraction result in slumping after sintering, hence, the amount of the liquid phase can be estimated from their corresponding phase diagrams based on the alloying content and designed accordingly. Apart from that, the other influencing factors when it comes to applying LPS for fabrication are the amount of additives/master alloy, particle size, shape, internal powder porosity, powder chemistry, homogeneity, green density, sintering conditions such as temperature, time, atmospheres, heating and cooling rates [52]. Hence, the selection of the activator or the liquid phase forming additives is such that it does not extensively dissolve in

the base material for shrinkage to occur. The importance of the master alloy is discussed in the following subsection.

3.7.1 Master alloys

Introducing elements through master alloy addition to obtain a liquid phase at a temperature well below the sintering temperature is the primary approach. Master alloy additions to PM steels were studied by Zapf et al. [54] at the beginning of the ’70s using Mn-Cr-Mo additions, and they found that this gave better mechanical strength considering the very low addition of alloying elements. Master alloys in ferrous PM steels have then been widely studied using different alloying additions, mainly based on the phosphorus and boron compounds, which form eutectic at low temperatures. One critical consideration during sintering is the preservation of the dimensional stability of the component. For this reason, a tailored master alloy approach is well suited [55]–[57], and boron addition is of particular interest and is addressed in this thesis.

3.8 Hot pressing

Hot pressing (HP) is one of the pressure-assisted sintering techniques, in which the powder is consolidated by the uniaxial pressing, while the die is also heated externally by the radiation from surrounding heating elements. The typical pressures that can be applied are between 25–100 MPa and full densification is reached after holding at the sintering temperature [49]. The processing can be performed in vacuum conditions to avoid any contaminations.

3.9 Spark plasma sintering

Spark plasma sintering (SPS), also known as field assisted sintering technique (FAST), is very similar to the HP, the only difference is in the heating system. The sample is heated by the Joule effect generated from the pulsed direct current applied through the die and a sample, which is conductive and allows for a high heating rate of 1000 °C/min [58]. However, the maximum pressure that can be applied is limited to 100 MPa due to the nature of the die, which is usually made of graphite. The SiC dies are used when higher pressures are employed, but this is associated with higher cost. The SPS allows for full densification of the components in a very short time, that is also restricting grain growth.

3.10 Additive manufacturing

Additive manufacturing (AM) is a process where the component is fabricated from a 3D CAD model where the material is added layer by layer. The AM offers flexibility in manufacturing as components with complicated features and shapes can be manufactured without tooling and with lower material waste. The AM processes that utilise metal powder are classified into powder bed fusion (PBF), direct energy deposition (DED), binder jetting (BJ) and fused filament fabrication (FFF) processes. Both the PBF and DED processes involve melting of the powder, whereas the BJ and FFF process involves shaping them through binder addition and subsequent sintering to form the metallic bonds.

3.11 Hot isostatic pressing

Hot isostatic pressing (HIP) is simply a heat treatment process under pressure, and the typical process involves simultaneous application of pressure and temperature to densify the material. The maximum pressure and temperature that can be reached are around 200 MPa and 2000 °C for most of the commercially available HIP presses. The pressure applied is homogenous which

allows for isotropic shrinkage and the dominant densification mechanism is through diffusional creep. At the end, there is however always normal diffusion to eliminate the last finite porosity. The main drivers and the applications are in nuclear, aerospace, oil and gas industries, where the demand for high-performance and safety requirements are extreme. HIP is also widely applied as a post-treatment process in the case of MIM and AM components.

Figure 10 shows the illustration of the typical process that takes place within a HIP chamber, where usually argon is used as a pressurising medium. This process is used to eliminate pores and defects in castings, diffusion bonding of dissimilar metals, revive used jet engine parts, consolidate powder, densify metallic composites, infiltrate and densify powder-based components [59], [60]. In addition to reaching full density by eliminating the pores, the performances of the HIP components are improved significantly – for example, the scatter in the properties are reduced in castings and for powder-based HIP materials the mechanical properties are increased owing to the full density and refined homogenous microstructure without any segregation [61].

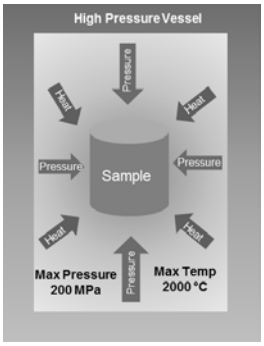

Figure 10: Illustration of the HIP process.

Powder consolidation through HIP involves preparation of capsules, powder filling, capsule sealing and removing the capsules, as shown in Figure 11 (a). The capsules are prepared to near-net shape or a preform of the final component. The powder is filled into the capsule which is made either from the same material as the powder or mild steel. The capsules are further evacuated, hermetically sealed and placed in the HIP chamber. After HIP, the powder is densified into a single piece of material through the combined mechanisms of yield, creep and diffusion. The capsules are removed after HIP, either through acid pickling or by machining, which is usually more time consuming and not economical for mass production. The main advantage of the powder-based HIP is the possibility to produce huge size components of several tonnages. In case of ingot metallurgy challenging to process alloys can be made by HIP [60].

3.11.1 **Capsule-free hot isostatic pressing**

Though the idea of performing capsule-free or container-less HIP has been proposed earlier [62], its potential for reaching full density in powder metallurgical steels is not fully exploited but is of enormous interest [15]–[17], [26], [63], [64]. Utilising capsule is economically viable only when it is used for large size components – more than 5 kg, and expensive component made of high alloyed powder such as tool steels, stainless steels, and superalloys. Hence, for smaller size and complex-shaped components required in high volume, the use of capsules is

not practically and economically viable for performing HIP. It has been estimated that just by avoiding the capsules, about 50 to 90% higher throughput can be realised [62]. In addition, recent developments in the HIP furnace system allows for combining rapid cooling and quenching. This reduces the HIP processing time and allows to avoid an additional heat-treatment (HT) as that can be combined into a single HIP cycle [13], [65]–[67]. A recent investigation has revealed that performing a normalising treatment within the HIP can reduce the grain size which was coarsened during the HIP cycle [68]. In addition, cooling can be accelerated with the influence of pressure in the HIP furnace [67] and this can further prevent any distortions or cracks that may arise during rapid quenching by preventing the formation of brittle phases. Additionally, the possibility to perform vacuum sintering within the HIP furnace before the HIP cycle (sinter+HIP) [62] and then the post heat treatment (sinter+HIP+HT) provides an enormous potential for the development of fully dense PM steels in a single process.

Capsule-free HIP for PM components is already applied for securing full density in the case of MIM and AM parts [69]. Usually, full density is not readily attained during sintering and a maximum of 98% can be achieved for a wide range of materials [62]. The pre-sintered parts with density >95% are necessary to maintain the pore closure on the surface for performing the capsule free HIP [6], [14]. Otherwise, the surface-open pores will not be closed after HIP, as observed in Figure 11 (b), and if the surface open pores are interconnected – it will not allow the material to densify.

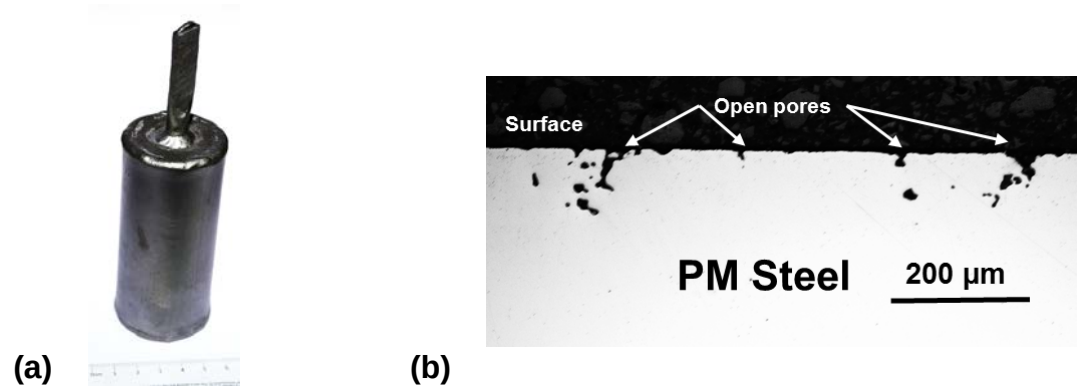

Figure 11: A typical HIP capsule filled with powder and sealed (a), micrograph from the surface of the PM steel after capsule-free HIP (b).

When it comes to the HIP of water atomised powder, the primary challenge originates from the oxygen present on the powder surface, which has to be reduced [70]. It should be noted though that the level of surface-bound oxygen for annealed water atomised steel powder is not a result of significantly thicker overall oxide thickness compared to that of gas atomised steel powder. It is merely a result of the much higher specific surface area owing to its more irregular shape. As it is known from the HIP of gas atomised powder, the presence of surface bound oxygen may result in the formation of fine oxide particles at the prior particle boundaries (PPBs). These sites may further grow in size or become the preferential sites for the precipitation of carbides and nitrides, which might influence the properties. The other challenge in powder-based HIP is the presence of Ar-induced pores that will apparently be reduced in size or closed during the

HIP, but tend to re-grow during the post-HIP heat treatment [71]–[73]. The reason being the fact that Ar is basically insoluble in metal. Another interesting phenomenon that occurs during the capsule-free HIP is the surface oxidation due to the interaction of processing gas (Ar) with the surface. The argon gas comprises a few ppm of oxygen and under high pressure it can lead to some surface oxidation which can be seen as a discolouration [74]. When using a HIP-capsule, this does not constitutes a drastic challenge as the capsule is removed, whereas the application of capsule-free HIP of course sets further demands on HIP atmosphere control. Even though there are several challenges, as outlined, the possibility of attaining full density in low alloyed PM steels in a robust and economically feasible way opens up a new area of the high-performance applications where low alloy steel fabricated from water atomised powder is not yet applied. Moreover, the implementation of the several hybrid approaches as presented in this thesis study will enable the manufacturing of fully dense and large-sized components.

4 FACTORS INFLUENCING DENSIFICATION AND ATTAINABLE PROPERTIES

In this chapter, the different factors that influence the densification and resulting properties after various stages of consolidation process are introduced and discussed.

4.1 Theoretical density of the powder mix

The theoretical density or the pore free density (PFD) of the powder mix is calculated based on the specific density and percentage of individual constituents present in the premix, including lubricant, metal additives and graphite. To estimate the PFD of powder mix, containing lubricant and additions as, e.g., graphite and fine powder of alloying elements, the general equation (8) can be used:

$$\frac{1}{\rho_{admix}} = \frac{w_g}{\rho_g} + \frac{w_l}{\rho_l} + \left(\frac{1 - w_g - w_l}{\rho_b}\right) \qquad (8)$$

Where w_g, w_l and ρ_g, ρ_l represents the weight fraction and specific densities of the admixed graphite and lubricant, respectively. Whereas, ρ_b is the specific density of base iron or steel powder. Let us consider steel powder pre-alloyed with 1.5 wt.% Mo (so-called Astaloy Mo), admixed with 0.6 wt.% lubricant and 0.2 wt.% of natural graphite. For this powder, the specific density ρ_b is around 7.89 g/cm^3, based on the pycnometer measurements. In this case, there seems to be no difference between the density of solid solution and that of individual mixtures, which fulfils Vegard's law as confirmed by Wever and shown by Liersch et al. [75]. Theoretical calculations show that the powder mix with graphite and lubricant can be pressed or compacted to a maximum green density equal to the pore-free density level as shown in Table 1.

Table 1: The maximum theoretical density of the powder mix calculated from equation 8.

Powder Mix	**Maximum density, g/cm^3**
Astaloy Mo+0.2 wt.% graphite	7.85
Astaloy Mo+0.6 wt.% lubricant	7.58
Astaloy Mo+0.2 wt.% graphite+ 0.6 wt.% lubricant	7.54

In the green compacts, to avoid cracks and delamination after pressing, maximum 98% by weight of the PFD is recommended [8]. Hence, compaction pressure should be optimised for such density levels. In the case of Astaloy Mo with 0.2 wt.% graphite and 0.6 wt.% lubricant, the maximum density level of 7.4 g/cm^3 is hence the optimum to avoid defects or failure after pressing.

4.2 Powder size and shape

The size and shape of the powder have a significant impact on the powder packing characteristics by affecting the flow, packing and compressibility [76]. In the case of PM steels, utilising water atomised powder which is irregular in shape, the standard powder size fraction is between 20 and 180 µm [77]. Having such a wide particle size distribution enables the smaller particles to fill the voids in between the larger particle, which improves the powder packing density. Still, having narrow powder size distribution affects the compressibility due to the poor packing behaviour and results in lower green densities. Larger content of the smaller sized

fraction creates more internal friction between the metal particles [76], which eventually requires a higher amount of energy to eject the compact from the die [43].

The shape of the metal particles determines the resulting green strength, where the irregular powder morphology promotes enhanced green strength owing to the interlocking of the metal particles upon pressing. This behaviour is apparent for the sponge iron powder contributing to better green strength than that of the water atomised counterpart, even though it has poor packing characteristics. It is similar for the case of gas and water atomised powder, which are spherical and irregular in shape, respectively, as shown in Figure 6 (a & b), where the irregular morphology results in a better green strength, even though the compressibility is better for spherically shaped powder [43], [78].

Having smaller powder size is expected to activate the sintering due to the excess free energy from the larger specific surface area. For the fine spherical powder between 1 to 20 µm being used in MIM applications, even if the initial solid loading is limited to around 60 vol% in the MIM stage, such powder size means that the material sinters to above 95% of the relative density [79].

4.3 Effect of the alloying elements

4.3.1 Compressibility

The effect of the alloying elements on the compressibility has to be taken into account as well to achieve good densification. The solid solution strengthening is known to play a significant effect on powder hardness and hence influence powder compressibility. For example, pre-alloyed powder depending on the effect of specific alloying element, require higher compaction pressures to achieve the same density level due to the solution hardening of the ferrous particles (hardening of ferrite) by alloying elements. In addition, powder particle size distribution, presence of internal oxides and fine-grain powder microstructure also tends to affect the compressibility [43], in some cases even more than expected based on the solution hardening of ferrite.

4.3.2 Role of boron during sintering

In PM steels, boron is an attractive alloying element and is added in large quantity as compared to the wrought steels. It acts as a sintering enhancer and enables liquid phase formation and promotes densification [16]. Based on an initial investigation by Klein et al. [80], relative density levels of 99.7% were reached for carbonyl iron powder sintered with 0.97 wt.% of boron. According to Madan et al. [81], boron is a good sintering activator for iron, based on the electronic configuration, thermodynamic phase stability and grain boundary cohesion criteria. Boron addition enhances sintering by the eutectic reaction between Fe(γ) and Fe_2B at 1175 °C, forming a liquid phase. Due to the unipolar solubility, iron will dissolve in the liquid and not the other way around as the boron has extremely low solubility in Fe. As a result, more liquid will be generated once the iron dissolves in the liquid, which will have a persistent character with an excellent wettability and a dihedral angle of less than 10° [82]. As a result of strong capillary action, the liquid will penetrate the particle boundaries and inter-particle regions with ease and finally impregnate into the grain boundaries. It causes the overall shrinkage by the primary and secondary rearrangement of metal particles, as illustrated in Figure 8 (a). The liquid phase will act as a short circuit path for iron diffusion, which eventually results in densification.

Recent studies have shown that by increasing boron content the density increases, which improves the strength and hardness but lowers the ductility [81], [83]. Selecká et al. [84] have shown that boron addition of up to 0.2 wt.% results in no significant increase in the density of Fe and Fe-Mo materials when sintered at 1200 °C for 60 min. There is a substantial increase in the density only when boron is added beyond 0.2 wt.%, which allows for more liquid phase formation. This also results in an increase in hardness due to the formation of a continuous boride network along the grain boundaries, which is extremely brittle. Boron is added either as an elemental powder, ferroboron or as a master alloy mix in a range of 0.01 to 1.2 wt.% of boron. The appropriate alloying method should be chosen to obtain the maximum utilisation of its liquid phase sintering effect. Even though the boron addition increases the density, several studies have shown the issue with the microstructural embrittlement that persists. [82]. Adding boron as a master alloy addition has been studied extensively for ferrous steel and stainless steel 316L and the reports have shown enhanced densification in combination with high ductility and surface densification [24], [55], [57], [85], [86]. Studies have shown that the different alloying elements present in the steel have significant influence through various interactions with boron, especially with Mo, Cr, Ni, and C, and are discussed in the following subsections.

4.3.2.1 Molybdenum

Molybdenum as an alloying element is added to increase the hardenability and in PM steel it is usually pre-alloyed. Elemental boron to the Mo-alloyed PM steel lowers the liquid forming temperature and forms higher liquid volume fraction at the sintering temperature [87], [88]. Further, with the presence of 3.5 wt.% Mo, the liquid formation temperature shifts to a higher temperatures but increases the amount of liquid resulting in an enhanced densification [89]. Karwan et al. [90] has shown that with 1.5 wt.% Mo, the addition of boron content up to 0.2 wt.% displays better ductility and beyond that embrittlement occurs through the formation of a hard phase.

4.3.2.2 Nickel

Nickel addition to PM steel has been of significant interest when it comes to the mechanical properties providing excellent strength and ductility suited for high-performance applications. In the ordinary steels containing boron, presence of Ni increases the boron diffusivity in γ-Fe similar to the behaviour of carbon in the presence of Ni [91]. Still, in the case of boron-containing PM steels, only limited studies have been performed. Introducing boron in the presence of Ni have improved the strength and hardness without comprising the ductility when boron content is up to 0.05 wt.%, but no influence on the density was shown [92]. Moreover, when boron is introduced as a master alloy with Ni (Ni-Fe-B mix) to the Fe-C and Fe-Mo-C matrix, with the addition of up to 3 wt.% MA, this enhances the density by around 2.4% with well-developed sinter necks [93]. Recent investigations have shown that the Ni addition reduces liquid phase formation temperature and aids in densification without segregating to the borides [94], [95].

4.3.2.3 Chromium

Chromium addition in Fe is of significant interest to increase the hardenability and in PM steels it is usually pre-alloyed due to its higher oxygen affinity. In the case of stainless steels, when the Cr content is varied from 11.8 to 30 wt.%, the liquid phase formation is suppressed [86]. In

the case of ferrous PM, increasing the Cr from 1.5 to 3 wt.% improves densification [94] but shifts the LP formation to a higher temperature [96].

4.3.2.4 Carbon

Infiltration of iron-carbon compacts with different materials based on the Fe-B system (ferroboron) has been studied for making composites with very high hardness [97]. Addition of carbon exhibits the material embrittlement, forming complex borocarbides which are detrimental to the performance of the material. The impact energy falls to extremely low levels of impact energy values (< 10 J/cm^2).

4.4 Influence of density and porosity on the properties

Numerous studies have shown the influence of density on the properties of PM steel and it is a limiting factor for applications. Based on the summary and review of all the previous studies, Beiss et al. [98] have derived the following general empirical relation (9) to estimate the PM steel properties in relation to density:

$$P = P_0\left(\rho/\rho_0\right)^m \qquad (9)$$

where P is the property of the PM material, P_0 is the property of the pore free material, ρ is the density of the PM material and ρ_0 is the theoretical density of pore free state. The value of exponent m depends on the measured property and the processing conditions.

Having full density provides a significant advantage for enhancing the properties and the performance of the components. Also, Figure 1 summarises the effect of the density on the mechanical properties in dependence on different processes, showing an increase in all cases with increasing relative density. Numerous studies [7], [99]–[101] have shown the effect of increasing density on enhancing the PM steel properties. In the high-performance applications such as gears, fatigue properties play a crucial role, and even the presence of few inclusions tends to be detrimental for the performance of the gear wheels. Hence, the presence of the pores in the PM steels will have an unprecedented effect on the material properties as they result in stress concentration regions. Therefore, the major issue with PM steel is, of course, the pore characteristics, i.e., amount of pores, pore size, their distribution and morphology [102]. The higher the sintered density or smaller the pores size, the lower will be the effect on the fatigue properties.

The strength of the PM material is related to the load bearing area that in turn is typically governed by the extent and characteristics of inter-particle necks. A model developed for predicting strength evolution considering the inter-particle neck size showed an excellent correlation with actual mechanical properties [103]. The neck formation starts with the inter-particle contacts and grows with increase in temperature, forming a continuous network. Through diffusion, inter-particle necks are formed, and stronger necks denote better mechanical properties [104]. This kind of characteristics can be assessed using the analysis of the fracture surfaces of tested sintered specimens [104], [105]. Higher initial density promotes better contact between the metal particles, lowering the porosity and improves the load bearing capacity.

4.4.1 **Open and closed porosity**

The open and interconnected pores are dominant when the porosity level exceeds 5%. They also have a more significant effect on mechanical properties than isolated and closed pores. This is due to the fact that the fatigue cracks initiate and grow through such pores and pore clusters [102]. While considering sintering to higher sintered densities, there is a concern when reaching porosity levels less than 5%, where the interconnected porosity practically ceases. This also means that gas transport inside the sintered part is limited and hence there is a risk of not reducing the surface oxides. Pores are the essential features for the efficient removal of products of lubricant decomposition and enable the escape of gaseous products (like water vapour) during the early reduction of iron oxide, required for the formation of inter-particle necks. When it comes to corrosion resistance, the presence of open pores at the surface tends to be a concern as well. The post-sintering heat treatment of PM parts like carburising or carbo-nitriding when carried out in the presence of open or interconnected pores results in deeper penetration of active gas, forming inconsistent case depths [106].

4.4.2 **Functional aspects of pores**

Another exciting aspect of the PM components is its ability to trap the lubricants owing to characteristic pores that provide improved frictional and wear properties [107]. Studies have shown the influence of the pore size in case of mating gears [108]. With the presence of larger pores in PM gear surfaces, damage due to scuffing and peeling occurred on the mating surfaces. Hence, it was recommended to have smaller pore size when using PM gears for best performance. Studies have also shown that having smaller average pore size of around 12 µm tends to increase the toughness of the PM steel by almost 25% [109]. To improve the fatigue properties of PM gears, considering tooth root failure, selective densification of gear sections and surfaces such as tooth and the flank have been employed. It was shown that gear rolling or surface rolling can be used to increase the load bearing capacity leading to surface densification of the PM gears [110]. This, in turn, improves the fatigue properties that becomes almost similar to the wrought material. The advantage of the PM gears is their ability to reduce the noise during operation which improves the noise vibration harshness (NVH) parameter.

4.5 **High-temperature sintering**

In terms of press and sinter, the final dimensions are usually fixed in the compaction stage itself and the distortions that arise from sintering are within the tolerance limit. This is because the sintering occurs in the solid state only to impart strength through the formation of metallic bonds. Densification of up to 1% is achieved when sintered at a high temperature > 1200 °C or in the case of liquid phase sintering, where the density is enhanced significantly. Haynes et al. [111] have shown how the properties of the sintered compacts made of pure iron powder vary with sintering at low and high temperatures. The results indicate that compacts made of pure iron powder at fixed density exhibit better mechanical properties either with increasing sintering time or temperature. This is supposed to be a result of the reduced stress concentration owing to the rounding of pores. Sintering at around 1120 °C is a standard industry practice for the majority of PM components. The reasons being that industrial belt furnaces are limited in application to around such a temperature, while there is also a concern not to apply too high temperature to maintain proper tolerance control of sintered parts.

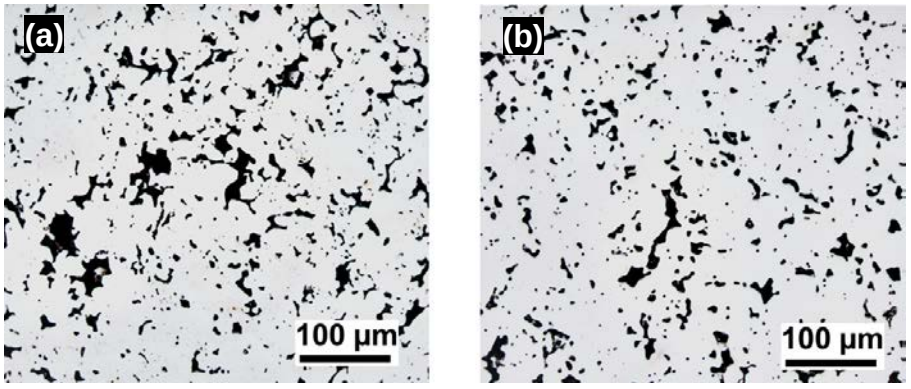

Figure 12: Optical micrograph of Cr-alloyed PM steel sintered at 1120 °C (a) and 1250 °C (b) in $N_2/10H_2$ atmosphere starting with a same green density of 6.8 g/cm^3.

The higher the temperature, the higher is the diffusion rate, which eventually results in an increased bonding and hence forming stronger inter-particle necks. This will result in an significant increase in strength of the PM steels [21], [112]–[114]. At higher temperatures, lattice diffusion also becomes significantly improved and this plays a major role in alloy homogenisation, which is essential in particular for the case of admixed and diffusion alloyed PM steels. Sintering at higher temperature is also beneficial for more efficient oxide reduction since the equilibrium for oxide reduction is shifted to higher oxygen partial pressures with increasing temperature. This fact is of particular importance in case of PM steels containing alloying elements like Cr, Mn, and Si, all prone to form stable oxides. Another important effect of the high-temperature sintering is the rounding of the pores compared to the conventional sintering temperature, see for example Figure 12 (a & b), and well developed inter-particle necks, which results in a significant improvement in the strength, especially fatigue properties of PM components [115]. The drawback with high-temperature sintering may be that there is some marginal shrinkage during sintering and hence dimensional control could be affected. At high temperatures, the reduction is governed by the carbothermal reduction processes via the initial presence of admixed graphite. Therefore, to enable the effective reduction, it is important that the necessary microclimate conditions are created early during the sintering. Sintering in vacuum at elevated temperatures is an another alternative to consider for large components with high densities [116], [117].

4.6 Effect of surface oxides on the performance of PM steels

Typical water atomised iron or steel powder, due to their much higher specific surface area for a given particle size, will have higher oxygen content as compared to that of gas atomised powder. Oxygen content in the water atomised powder is determined by the alloy composition and post-atomisation annealing process applied. In the case of Cr-pre-alloyed powder, powder surface is covered by a homogenous iron oxide layer with the thickness of 6 to 7 nm or even smaller and islands of oxide particulates rich in Cr, Mn, and Si [23], [35], [36]. The surface iron oxide layer covers more than 90% of the powder surface [118] which accounts for about half the amount of total oxygen content. In addition to the initial bulk oxygen content of the powder, there is a risk of further oxidation, mostly from the powder handling and improper atmospheric control during sintering [119]. Still, the key aspect is the much higher specific surface area and

not the oxide thickness of the water atomised powder which is of same order of magnitude as in case of gas atomised powder.

As discussed earlier, the formation and growth of the necks determine the strength of the PM steels. Therefore, the oxides on the powder surface need to be reduced during the sintering process to enable early formation of inter-particle necks [120]. If the surface oxides are not reduced at an early stage during sintering, they will transform to more stable oxides, and eventually coarsen at the expense of sintering temperature and time [121], [122]. Hence, there will be particulate oxides at the necks that may inhibit the development of good inter-particle bonding [123], which in turn adversely affects the mechanical properties [36].

In addition to the sintered steels, the studies of powder-based HIP of stainless steels have shown that there is a significant influence of oxygen content on the mechanical properties, mainly on the impact energy values [124]–[126]. Crucial is the fact that the surface oxide on powder particles always constitute a source for the decoration of oxide particles on prior particle boundaries (PPBs), which in turn affects the mechanical behaviour of the material after HIP [127]. Furthermore, the initial Fe-rich surface oxide can transform to more stable oxides [70], [128]. Depending on amount of surface oxide, the amount and distribution of oxide particulates on the PPBs will also be triggered resulting in reduced toughness. This is confirmed by lower impact values as the PPB regions allow fracture to easily propagate [127], [129].

5 EXPERIMENTAL DETAILS

5.1 Materials and processes

Water atomised iron and steel powder grades, produced by Höganäs AB, were investigated within the scope of several studies. The chemical compositions of the studied water atomised powder grades are given in Table 2. The composition of the gas atomised Ni-Mn-B master alloy powder, developed by CEIT, Spain [24], [25] and produced by Höganäs AB, is also given in Table 3.

Table 2: Chemical composition of the water atomised powder grades in wt.%.

Powder base	Commercial name	Fe	Cr	Mo	C	O
Cr pre-alloyed	Astaloy CrA	Bal.	1.8	-	<0.01	0.15
	Astaloy CrM	Bal.	3	0.5	<0.01	0.15
Pure Iron	ASC100.29	Bal.	-	-	< 0.01	0.08
Mo pre-alloyed	X-Astaloy0.45Mo	Bal.	-	0.45		
	Astaloy Mo	Bal.	-	1.5	<0.01	0.07

Table 3: Chemical composition of Ni-Mn-B master alloy powder in wt.%.

Master alloy	Ni	Mn	B	N	C	O	S
Ni-Mn-B	46.00	46.10	7.90	0.001	0.075	0.025	0.004

The experimental matrix is summarised in Table 4, where the powder mixes being used are presented and the various type of specimens with different initial compacted densities and subsequent sintering conditions being used are shown as well. The powder mixes were admixed with lubricant, typically 0.6 wt.% of Kenolube and in some cases Lube E were used.

5.1.1 Compaction

Cold die compaction was used for consolidating powder to density levels of between 6.8 to 7.3 g/cm^3, with typical pressure being applied in the range of 550 MPa to 800 MPa. In the case of the double press-double sintering, the density of 7.5 g/cm^3 was reached from the initial density of 7.2 g/cm^3 by pressing at 800 MPa. This is mainly due to the remaining volume from the removal of lubricant after first sintering and annealing of the compact and hence softening the material, which assists significantly to the further compaction stage.

5.1.2 Delubrication

All the delubrication trails were performed at 450 °C in a dry nitrogen atmosphere in the laboratory tube furnace Entech with a dewpoint of -45 °C. In case of the industrial sintering trails, the de-lubrication was performed in the continuous furnace in the delubrication zone. In the case of double pressing-double sintering approach, the delubrication is performed during the same stage as specimens annealing that was done at 800 °C for 30 minutes in nitrogen, to relieve the stresses and anneal the material before the second stage of compaction..

Table 4: Summary of the experimental matrix used in the scope of this thesis.

Paper No	Powder mix	Graphite, wt.%	Test specimens	Densities g/cm^3	Sintering temperature - time, °C-min	Atmospheres
I	Astaloy CrA	0.60	– IE bars (55x10x5 mm^3)	7.0	450 – 1 700 – 1 900 – 1 1120 – 1 1120 – 30	– N_2-10H_2
II	Astaloy CrA	0.45 0.75	– IE bars (55x10x10 mm^3)	7.1, 7.3	1120 - 30 1250 – 30	– Vacuum ($10^{-4,}$ 10^{-2}, 1, 10 mbar)
III	Astaloy CrM	0.50 0.55	– IE bars (55x10x10 mm^3) – Tensile specimens	6.8, 7.0 7.1,7.3	1120 – 30 1250 – 30	– N_2-10H_2 – Vacuum (~0.1 mbar)
IV	ASC100.29 (ref) Astaloy CrM	0.40	– Small cylinders (mould d=19 mm and h=27 mm)	3.0 to 7.5	1120 – 30 1250 – 30	– Ar-10H_2 – N_2-10H_2 – Vacuum (~0.1 mbar)
V, VI	ASC100.29 (ref) X-Astaloy0.45Mo 1.5 and 2.5 wt.% of MA	0.30	– IE bars – (55x10x10 mm^3)	7.0, 7.3	1000 – 1 1100 – 1 1240 – 1 1240 – 30	– Ar-50 H_2 – 100 H_2
VII	Astaloy Mo – standard fraction (20-180µm) – fine fraction (< 63 µm)	0.20	– Cylinders (d= 25 mm, h=20mm) – Gears (m=1.58mm, d=31.75 mm, w=10 mm)	7.2 7.45 - 7.5	800 – 30 1250 – 60 1300 – 60	– N_2 – Vacuum (~0.1 mbar)

5.1.3 **Cold isostatic pressing**

For the CIP trails, silicone rubber tubes of 19 mm in diameter and 27 mm height were used as mould, which was sealed at both the ends with a graphite sealant. After powder filling and sealing, the moulds were vacuum sealed in a polythene bag, as this not only evacuates the air but also avoids the pressurising medium (water or oil) in contact with the mould. All the CIP trails were performed at Quintus Technologies AB, Sweden, utilising a Q170 wet bag CIP press, having maximum capacity of 1200 MPa with a pressure uniformity of ±1 MPa at steady state conditions. The size of the CIP chamber is such that eight moulds of the above-specified dimension can be pressed in each cycle. The pressure was between 100 to 800 MPa for all the studies, with a hold time of 120 seconds per cycle.

5.1.4 **Sintering**

Sintering trails were performed in a laboratory tube (quartz) furnace Entech at 1120 °C using 90% N_2/10% H_2 with a dewpoint of around -50 °C. All the liquid phase sintering trails were performed in dilatometer DIL 402C from Netzsch in Ar/50%H_2 atmosphere at a temperature of 1240 °C. In the case of vacuum sintering, the different levels of vacuum (10^{-4}, 10^{-2}, 1, and 10 mbar) were used in the same dilatometer at 1120 °C and 1250 °C. All the industrial sintering trials were performed at Höganäs AB using the continuous sintering furnace at 1120 °C and in some cases case followed by sinter hardening during cooling with a typical cooling rate of 3 – 5 °C/s. High-temperature sintering was also performed in the batch furnace in N_2/10H_2 at 1250 °C. All the vacuum sintering trials were performed using an ECM furnace at ~ 0.1 mbar, followed by forced cooling with a cooling rate of 4 °C/s.

5.1.5 **Hot isostatic pressing**

In the case of powder-based HIP, Cr-alloyed steel powder (Astaloy CrM) with and without graphite was encapsulated in a mild steel capsule of 70 mm in diameter and 120 mm height using electron beam welding under high vacuum at Forschungszentrum Jülich GmbH. The HIP cycle was performed utilising a QIH-9 URQ from Quintus Technologies AB, Sweden, at a facility in Ruhr-Universität Bochum. In addition, capsule free HIP trails were performed at Quintus Technologies AB in Västerås utilising QIH-21 HIP. The HIP cycles used for all the approaches included a HIP temperature of 1150 °C and 2 hours of holding time with an argon gas pressure of 100 MPa, followed by natural cooling.

5.1.6 **Heat treatment**

In order to correlate the properties of the sintered and the HIP specimens, a combined heat treatment was performed by heating to 960 °C in ~ 0.1 mbar of vacuum and cooling down at a rate of ~4 °C/s. Tempering of the samples after sintering and heat treatment was performed at 200 °C in air for 1 hour unless specified otherwise.

5.2 Analytical techniques

5.2.1 X-ray photoelectron spectroscopy

X-ray photoelectron spectroscopy (XPS) or electron spectroscopy for chemical analysis (ESCA) is a surface sensitive analytical technique, where the sample in ultra-high vacuum will eject the characteristic photoelectrons from the core shells of the atom once irradiated with the soft X-rays as given in Figure 13. The measured property is the kinetic energy of the emitted photoelectrons which can then be related to the characteristic binding energy and correlated to the element of interest, according to equation 10. The survey spectrum indicates the presence of elements within the analysed area. The high-resolution scan at the selected energy region at different etch depths provides the chemical states of the element, its distribution at different depths and also allows quantification of the surface chemical composition [130].

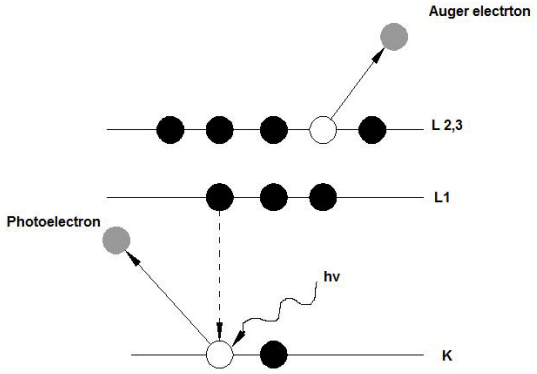

Figure 13: Schematics of the XPS principle, redrawn from [130].

$$KE = hv - BE - \emptyset s \qquad (10)$$

Equation (10) gives the kinetic energy of the emitted electron, where hv is the X-ray photon energy, BE is the binding energy and $\emptyset_S$ is the spectrometer work function. The binding energy is regarded as the ionization energy of an atom for the particular shell. Usually, ionization occurs to a depth of a few µm, however, only those electrons from the depth of tens of angstroms below the surface can leave the shell without the loss of energy. These electrons contribute to the peaks in the spectra. They are detected according to their kinetic energy by the electron spectrometer. In this study, XPS analysis was performed on the fracture surfaces using a PHI 5500 instrument using AlKα (hv = 1486.6 eV) source on an area of roughly 0.8 mm in diameter. Both, the survey and high resolution scans were captured for the selected elements, combined with the compositional depth profiling to the following nominal etch depths of 1, 3, 5, 7.5, 10, and 20 nm using Ar ion etching. For the calibration of the depth profiling, Ta_2O_5 foil with the known thickness of Ta_2O_5 oxide was used and hence the etch depths refer to Ta_2O_5 units.

5.2.2 Scanning electron microscopy

As the resolution of the optical microscope is limited by the wavelength of the light, for high-resolution imaging scanning electron microscopy (SEM) is necessary. Hence, this is one of the most common analysis tools used for material investigations. The principle of operation is based

on the scattering of electrons (elastic or inelastic) when the electron beam from the source (e.g., W, LaB_6 or FEG) interacts with the material. The information obtained is defined by the interaction volume that is determined by the accelerating voltage. For topographic information, secondary electrons (SE), which originate from the surface due to the inelastic scattering were used. For the elemental contrast between different elements or phases, the backscattered electrons (BSE) are used. Apart from imaging, the characteristic X-rays emitted from the material upon interaction with the electron beam, allows for both qualitative and semi-quantitative chemical analysis, using the energy dispersive spectroscopy (EDS). Information is obtained from the very top surface of the sample (a couple of microns) and to detect the lighter elements (like B, C, N, O, etc.), the low accelerating voltage might be of interest. In the case of high-resolution imaging, small working distances are also advised. In this study, Leo Gemini 1550 FEG instrument for high-resolution imaging is used for microstructural analysis in combination with the X-MAX EDX detector and Aztec software for chemical analysis. Qualitative and semi-quantitative chemical analysis was performed by point analysis and the elemental distribution was analysed by means of line scan and mapping. The fractographic investigations were conducted using Inlens and SE detectors with the accelerating voltage of 10 – 20 keV.

5.2.3 **Thermal analysis**

5.2.3.1 Differential scanning calorimetry

Differential scanning calorimetry (DSC) is a thermo-analytical technique which measures heat flow between the sample and reference material in a controlled temperature profile. Alumina crucibles with lids were used in this study: one for the samples and one as an empty crucible to record the difference in the heat flow. The energy absorbed or released associated with specific phase change such as crystallisation, melting and phase transformations are measured to determine the phase transformation temperatures and the specific heat capacity of the material.

In this study, simultaneous thermal analyser STA 449 F1 Jupiter® from Netzsch was used with the DSC sensor, which allows both, calorimetric and thermogravimetric measurements in a single run. All the trails were performed using high purity Ar gas atmosphere with heating and cooling rates of 10 °C/min.

5.2.3.2 Dilatometry

The thermal expansion or shrinkage associated with the phase transformations can be determined using the dilatometer by accurately measuring the dimensional change during a controlled temperature profile. As the sintered properties are affected by the heating and cooling rate, it is essential to have a controlled process to simulate the actual conditions here. The DIL402C horizontal pushrod dilatometer from Netzsch equipped with W-Re thermocouple that can be used for reducing and inert atmospheres was applied in this study. The dilatometer was equipped with vacuum-tight SiC furnace and is connected to the rotary and turbopump that allows performing sintering in vacuum of down to 10^{-5} mbar. It is possible to have an excellent atmosphere control and flexibility to change the atmosphere during the process with the help of a mass flow controller.

The sample is placed in the alumina sample holder and the push rod is pushed against the sample with a minimum force of 25 cN. The push rod is connected to the transducer that converts the linear displacement into electrical signals with a resolution of up to 0.125 nm or 1.25 nm, depending on the measurement range. Before starting the experiment, the dilatometer was evacuated and further flushed three times using high purity Ar gas and the program was set to begin with the appropriate atmosphere.

5.2.4 **Chemical analysis**

The bulk oxygen and carbon contents of the sintered materials were determined using LECO instruments of TC-600 and TC-844 type at Höganäs AB. The oxygen analysis was carried by heating the sample in a graphite crucible under the flow of helium gas. During heating, the oxygen from the sample will interact with carbon from the crucible, resulting in release of CO and CO_2 gas species, which are further captured by the IR detectors to determine the amount of oxygen content. For the carbon analysis, the sample is combusted in an induction furnace under the flow of oxygen, and the carbon from the sample will react with the oxygen forming CO and CO_2 gas species, which are again captured by the IR detector to determine the bulk carbon content.

5.2.5 **Density measurements**

Density measurements were done according to the Archimedes principle (ISO 3369). This was done by measuring the weight of the sample in the air first and measuring the weight of the sample in water using a special set up. The density of the sample was calculated according to the following equation (11):

$$\rho = \frac{m_a \times \rho_w}{m_a - m_w} \text{ (in g/cm}^3\text{)} \qquad (11)$$

Where m_a and m_w are the masses of the sample in air and water in gram and ρ_w is the density of water (1 g/cm^3). The samples were impregnated with paraffin wax to seal the open pores.

5.2.6 **Gas pycnometry**

Measurement by gas pycnometer provides the true density or the absolute density of the material utilising He or N_2 gas as the displacement medium. Helium is preferred mostly due to its ideal gas behaviour and has smaller molecular size. It can penetrate the smaller pores which are otherwise impregnable using water for example. In this study, He-pycnometer measurements were performed using an AccuPycII 1340 He-pycnometer at Höganäs AB. The analysis provides the pycnometer density value, which gives the amount of closed porosity and by subtracting it from the total porosity measured from the density after water displacement method, the amount of open pores was obtained.

5.2.7 **Light optical microscopy**

The light optical microscope is a basic yet powerful tool in the field of materials science. As the light source illuminates the surface of a sample, the reflected light is collected through the lenses forming the image. The digital camera can capture this image for further analysis. The image resolution is limited by the wavelength of the light and numerical aperture of the objective. In this thesis study, Leitz DMRX microscope equipped with a Zeiss digital camera

and AxioVision software for analysis is used. All the metallographic samples were polished and etched using 2 vol.% nital solution (2% of HNO_3 in ethanol) to reveal the microstructure under the light optical microscope. Porosity analysis was performed using ImageJ software on the as polished optical micrographs taken at 200x magnification.

5.3 Mechanical testing

All the mechanical testing trials were performed according to the PM standards. Impact testing was performed on IE bars prepared according to ISO 5754 to evaluate the impact energy values. Tensile testing was performed according to the ISO 2740 standard to assess the tensile strength, yield strength and the ductility. The analyses were performed on approximately 7 to 10 samples for each test unless otherwise specified. All the hardness measurements were done according to the PM steel standard ISO 6507-1. The apparent hardness measurements were carried using Wolpert Dia Tester with 10 kg. The micro-hardness was measured using Shimadzu HMV-2000 and loads used were typically between 50 to 100 g. When it comes to PM steel, the macro-hardness value measured is the apparent hardness, since it combines influence from both the bulk material characteristics and the inherent pores. When it comes to micro-hardness, the hardness of the individual grain, phase or particle is measured.

6 SUMMARY OF APPENDED PAPERS

Figure 14 summarises the approaches included in this thesis based on the appended papers (Paper I –VII) and categorises them into results for Cr-pre-alloyed and Mo-pre-alloyed PM steels, respectively. The main scope is to address the critical aspects involved during the processing of PM steels by utilising water atomised powder to reach full densification.

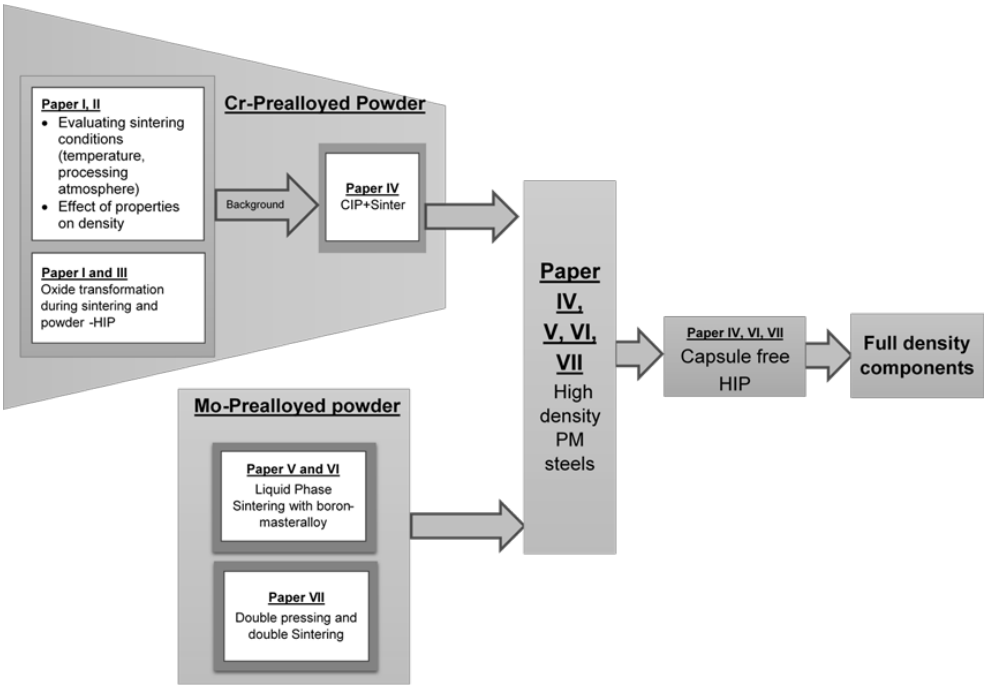

Figure 14: Summary of studied approaches based on the appended papers.

In this thesis study, to analyse the sintering behaviour of high-density PM steels in different sintering conditions, the effectiveness of sintering in different processing conditions: sintering temperature and atmospheres were investigated (Papers I and II). Besides, the mechanical behaviour was also analysed for the samples pressed to different initial densities (Papers I and II). The oxide transformation was analysed during sintering in the hydrogen-containing atmosphere (Paper III). The mechanisms involved in the oxide transformation during sintering and consolidation via powder HIP approach using encapsulation were also addressed (Paper I). All the studies on oxide transformation (Papers I, II, and III) provided the necessary background and addressed the challenges encountered in consolidating Cr-pre-alloyed PM steels. These results form the basis for full density consolidation via the following CIP→Sinter→Capsule free HIP approach (Paper IV). When it comes to Mo-alloyed powder, the liquid phase sintering utilising boron-containing master alloy is adopted to enhance the densification during sintering (Paper V) followed by capsule-free HIP (Paper VI) to reach full density. Paper VII contains the study on double pressing-double sintering (DPDS) approach to achieve high-density levels above 95% followed by capsule-free HIP for attaining full density. All the approaches which are mentioned in the appended papers are intended for achieving high enough density to enable surface pore closure during sintering, whereby capsule-free HIP can be applied to achieve full density.

6.1 Influence of processing conditions on sintering of Cr-alloyed PM steels

Sintering of Cr-alloyed steel samples in different processing conditions with special focus on sintering atmosphere and temperature utilising different density samples, are discussed in this section.

6.1.1 Hydrogen containing atmosphere

Sintering in hydrogen containing atmosphere is the most common practice in case of PM steels sensitive to oxygen, where reduction of the Fe-oxide takes place at a lower temperature around 450 to 550 °C. This early reduction enables formation and growth of inter-particle necks which are crucial for the properties of the PM steels. By utilising hydrogen in the early stage of sintering in reducing the iron oxides, the amount of carbon loss can be minimised and better carbon control can be established. The reducing ability of the atmosphere sintering is limited by the ability to penetrate the compact during sintering, which is influenced by the compact density being used. The higher the initial green density, the lower the atmospheric penetration into the component, especially when it comes to the removal of the reaction products from the pores inside massive components.

6.1.2 Effect of different vacuum levels

The initial investigation on the role of different levels of vacuum (10^{-4}, 10^{-2}, 1, and 10 mbar) during sintering in the lab environment (Paper II) showed that irrespective of the vacuum levels, the sintering is effective when performed at 1250 °C. The initial oxygen content of the base powder was about 0.15 wt.%, whereas sintering in different vacuum levels revealed almost complete oxide reduction for all the conditions with final oxygen content of less than 0.02 wt.%. The dominant reduction mechanism is through the carbothermal reaction, where the added graphite plays a major role during the vacuum sintering. This results in the carbon loss between 0.05 to 0.1 wt.% in dependence on the alloy system, vacuum level and sintering temperature. Hence, sintering in vacuum could be an alternative for atmospheric sintering providing the alternative in terms of reduction by forming local reducing conditions within the compact – “microclimate”. However, sintering in high vacuum levels lead to sublimation of Fe and Cr from the matrix and depositions on the furnace walls [117]. Nonetheless, such high vacuum levels are not feasible for sintering in an industrial furnaces. Hence, the trails were performed at vacuum levels of 1 mbar and 10 mbar. The samples with two different densities and carbon content were sintered at 1120 °C and 1250 °C and the mechanical properties and chemical compositions were evaluated. The results show that the irrespective of the vacuum level the sintering is effective in reducing the oxides up to 0.02 wt.% especially at high sintering temperatures, with significant improvement in properties.

6.1.3 Sintering temperature

Sintering temperature has a significant impact on the oxide reduction, porosity and the resulting mechanical properties. About 30 to 50% of the initial oxygen is reduced when sintering at 1120 °C, see Figure 15 (a). Sintering at 1250 °C reduces up to 70 to 80% of oxygen content compared to the initial amount of 0.15 wt.%. Hence, it is clear that increasing the sintering temperature from 1120 to 1250 °C has the most relevant effect on the oxygen content reduction, irrespective of the carbon content and density level. Sintering at a higher temperature contributes to more carbon loss as carbon is the only reducing agent in case of vacuum sintering. Hence, this must

be considered during initial design of the powder mix. Pores tend to transform from from open to closed and get more rounded. Hence, there is a slight increase in densification but there is more significant improvement in the properties.

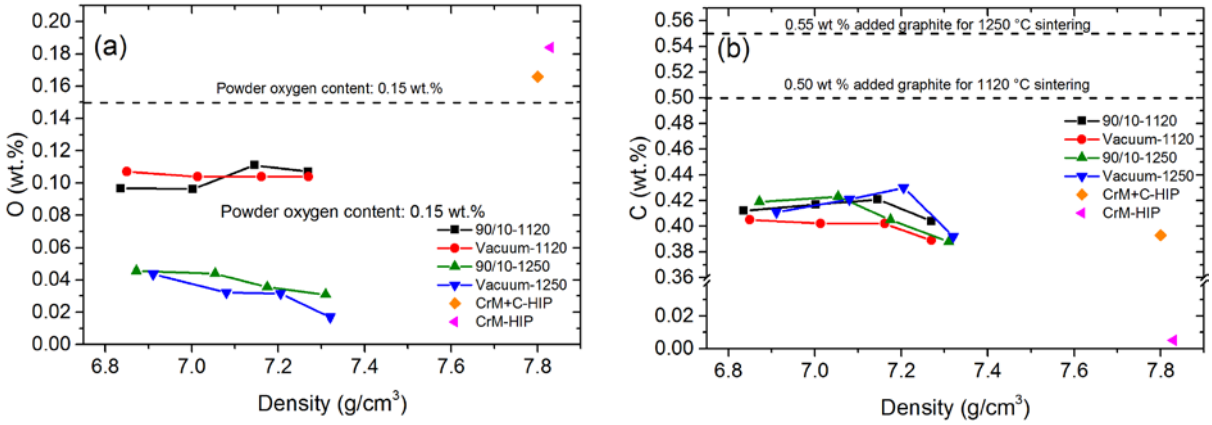

Figure 15: Chemical analysis of the sintered and HIP samples: carbon (a) and oxygen (b) content [Paper I].

6.1.4 **Density**

Increasing the density levels reduces the interaction with the sintering atmosphere due to the limited amount of open and interconnected pores. By investigating the samples with the different densities, the higher density samples exhibited slightly higher carbon loss than the lower density samples, see Figure 15 (b). The role of carbon is quite significant at higher sintering temperature, which reduces the oxyen content to as low as 0.02 wt.%. In general, it can be interpreted that for the high-density samples, higher sintering temperature is needed for either sintering in vacuum or in hydrogen-containing atmospheres, with the controlled graphite addition to compensate for the carbon loss during sintering.

6.2 **Effect of density on properties after sintering and powder-based HIP**

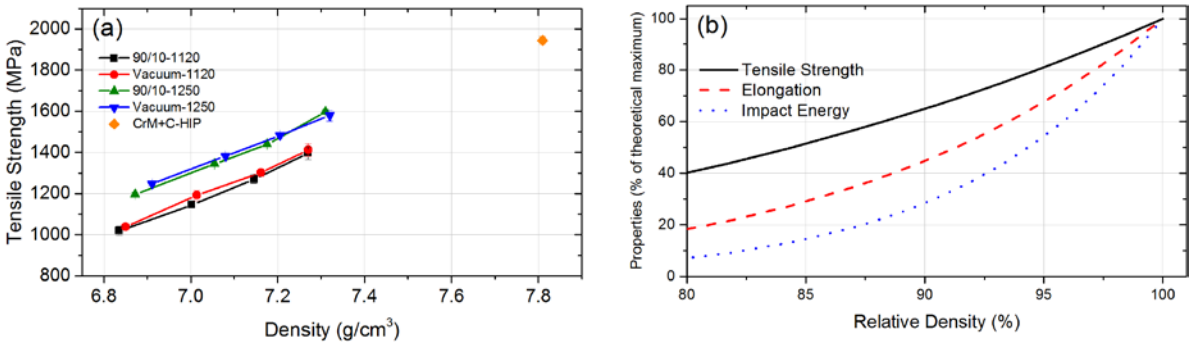

Figure 16: Density vs tensile strength (a), and effect of density on properties (b) [Paper I].

In Paper I, the samples with higher Cr content were utilised to understand the impact of sintering in different conditions, at different temperature and atmospheres, using samples with a different initial densities varying between 6.8 to 7.3 g/cm^3 see Figure 16 (a). To achieve the equivalent material properties after sintering, the initial graphite addition is varied to account for the carbon loss that happens during sintering so that that final carbon content can reach a nominal amount

of ~ 0.4 wt.%. The relation between density and properties is apparent as seen in Figure 16 (b), in which the mechanical properties are increasing significantly with the density. Powder-based HIP approach was also used alone to attain a fully dense PM steel as a standard reference for predicating the properties in the intermediate density stages. The model proposed in the equation (9) is applied for predicting the properties of the intermediate densities and the showed variation in the behaviour with respect to the different sintering conditions.

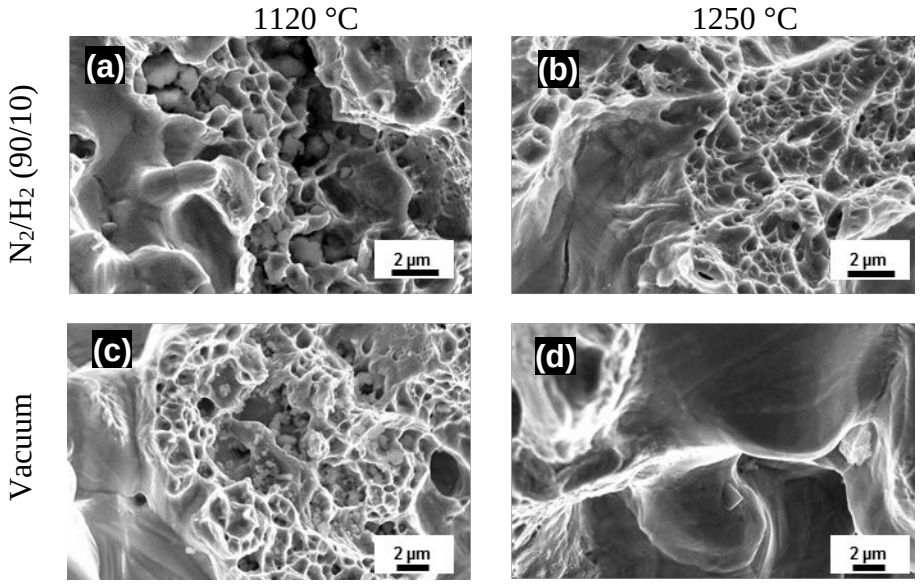

Figure 17: Fracture surface obtained after sintering at 1120 °C and 1250 °C for 30 minutes in 90N_2/10H_2 (a and b) and vacuum of ~ 0.1 mbar (c and d) [Paper I].

The analysis of the fracture surface of the sintered and HIP samples clearly reveals increase in inter-particle necks with increase in density. The particle surface appears to be clean irrespective of the sintering conditions and the fracture is mainly inter- and trans-particle ductile failure. The dimples are often initiated at oxide inclusions, with the presence of oxide inclusions within the fractured necks being a common feature observed for all the sintering conditions to various extent, see Figure 17. Significantly more oxide inclusions can be seen in case of low-temperature sintering whereas in case of high-temperature sintered samples oxide inclusions can be found only sporadically. In the case of HIP samples, fracture surface appears to be rougher with the presence of oxide inclusions all over the neck regions. It is evident that the failure takes places through these prior particle boundaries enclosing the oxides as they are the weakest volume of the material for the crack to propagate.

6.3 Oxide transformation during sintering and HIP

Sintering is a surface phenomena and the interactions that occur on the surface of the metal particles define the properties and performance of the PM steel and hence determines the limits of its application. Therefore, it is essential to analyse the oxide transformation that takes place during sintering of Cr-alloyed PM steels to have an understanding of proper process control. Paper III presents the XPS and SEM analysis on fracture surfaces of PM steel made from powder pre-alloyed with 1.8 wt.% Cr. The Analysis on the de-lubricated (450 °C for 30 min) fracture surface reveals that the surface characteristics are similar to that of the as-received powder, having a surface iron oxide layer of 6 to 7 nm in thickness and small particulate oxide

features rich in Cr, Mn, and Si. This shows that elements like Mn and Si are selectively oxidized to certain extent despite of theme present as trace elements. As the de-lubrication is performed in pure N_2 atmosphere at 450 °C, there is no change in surface oxide composition at such temperature and the initial powder characteristics are retained. However, further analysis reveals that the samples heated to 700 °C in the presence of hydrogen-containing atmosphere contributes to the surface iron oxide reduction.

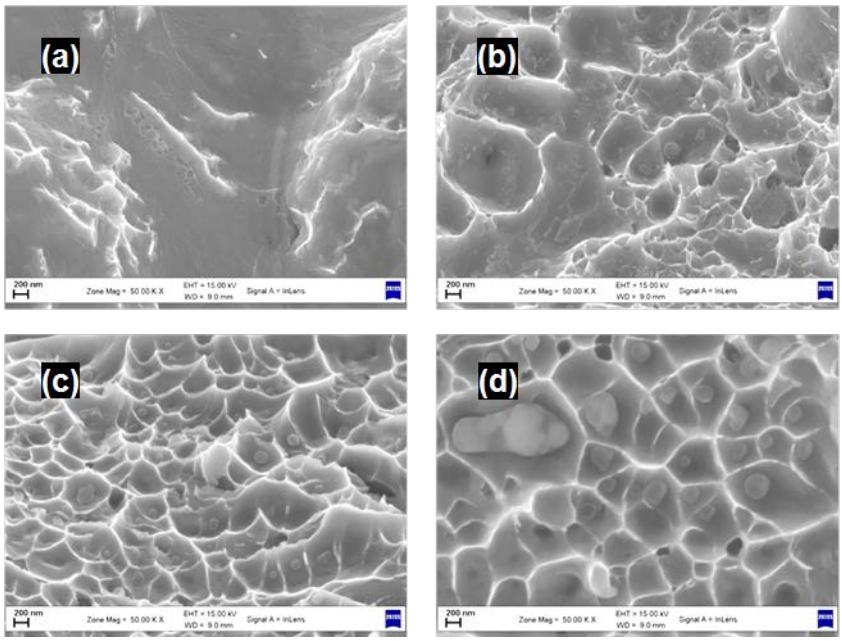

Figure 18: SEM micrographs showing the fracture surface of the Cr-pre-alloyed PM steel sintered at different temperatures: 700 °C-1 min (a), 900 °C-1 min (b), 1120 °C-1 min (c), and 1120 °C-30 min (d) [Paper III].

From the XPS analysis, the increase in the relative cation concentration of Cr, Mn and Si are observed after heating at the temperature range of 700 to 900 °C. Such increase indicates formation of oxides rich in these elements, even though again Mn and Si are present as trace elements. Hence, the temperature range in question is critical since the carbothermal reaction (both direct and indirect) will be active only above 800 °C, resulting in further reduction of the oxides. Furthermore, due to the nature of the reactions, the earlier growth and development of the inter-particle necks are significant for the effective sintering to take place.

The analysis of the fracture surfaces of samples heated at 700 °C and 900 °C for short nominal period of time (1 minute), see Figure 18 (a, b), shows the branches of neck formation, where the particle were supposed to be in contact and continued to grow with the temperature. The un-reduced oxide residues are hence entrapped in the forming necks with result of oxide particulates. The fracture surface in Figure 18 (c, d) indicates well developed inter-particle necks with ductile dimple features with the particulate oxides that tended to coarsen with the holding time during sintering. These particulate oxides are rich in Cr-Mn-Si, supposedly spinel oxide, its formation being consistent with thermodynamic stability assessment. Such kind of oxide is not entirely expected to be reduced during sintering temperatures of below 1120 °C

and hence increasing the temperature above 1200 °C should contribute to a significant reduction.

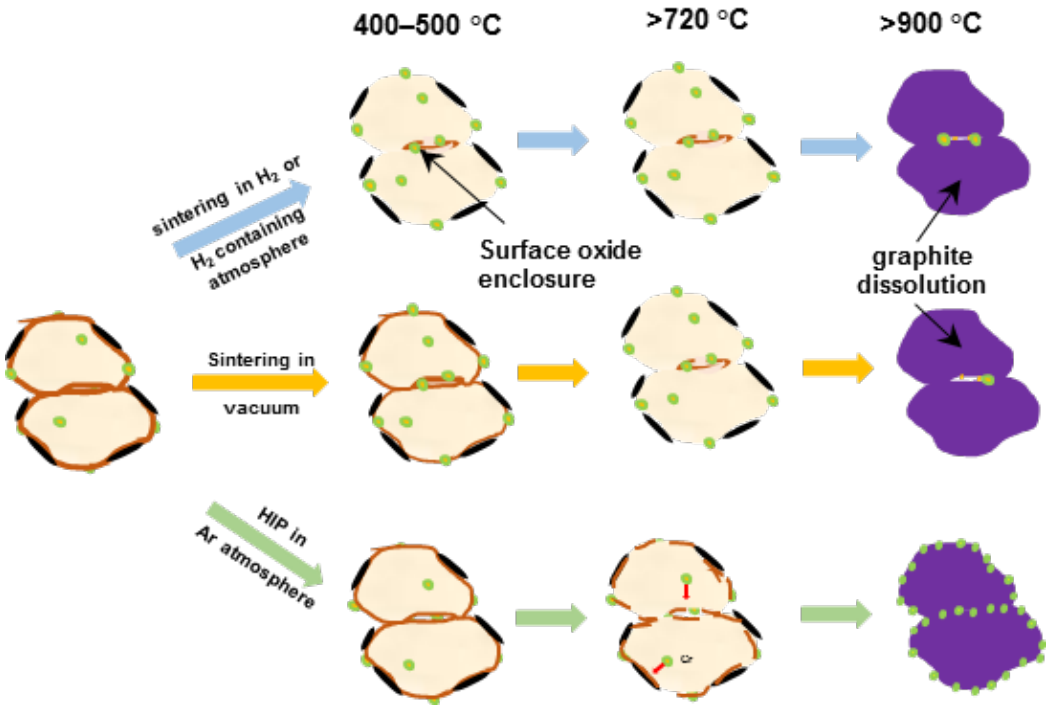

Figure 19: Model illustration of the oxide transformation that takes place during sintering in hydrogen-containing atmosphere, vacuum conditions and during HIP.

Sintering of water atomised powder involves initial reduction of the surface oxides to form the inter-particle bonding otherwise it will act as a diffusion barrier. The fracture surface indicates the degree of bonding that has developed during the different stages of sintering. In the vacuum sintering, there is no oxide reduction during the initial phase due to the absence of hydrogen. Carbon plays than a major role contributing to the reduction above 900 °C and its effect is more pronounced when sintered at high sintering temperatures. In the case of powder-based HIP, even though there is a presence of graphite, due to the closeness of the system oxygen cannot be removed from the material and hence chemical composition of the material (including carbon and oxygen) remains the same. Similar to the sintering, the surface iron oxides are transformed into more stable oxides rich in Cr, Mn, and Si along the prior particle boundaries. The main difference in case of oxide transformation during powder-based HIP is the significantly higher amount of oxide residues in comparison with sintering. Based on this, a model of oxide transformation is proposed, see Figure 19, illustrating different oxide transfomation mechanisms taking place under different conditions and it highlights that in the absence of reducing condition in the atmosphere all the iron oxides covering the powder surface are transformed in to more stable oxides according to the thermodynamic equilibrium.

6.4 Approaches for reaching full density

Figure 20 presents the different approaches considered in this study based on the appended papers in order to reach the full density in PM steel. All the approaches, including cold isostatic pressing, liquid phase sintering and double pressing-double sintering, enabled reaching the higher density levels through high sintering temperature. This allowed further utilisation of capsule-free HIP for full densification.

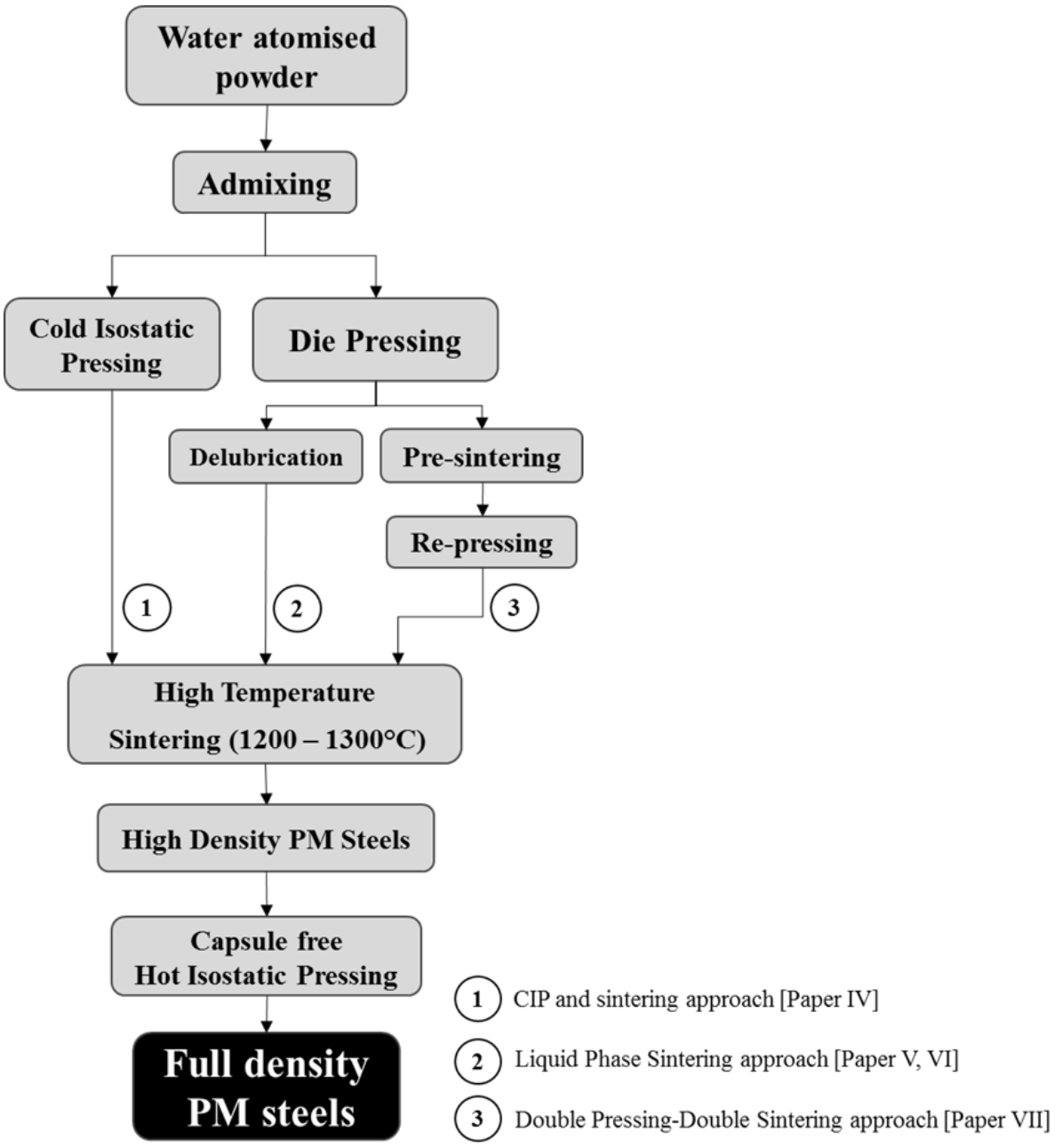

Figure 20: Process flow adopted for attaining full density in PM steel.

6.4.1 **Cold isostatic pressing with subsequent sintering**

The investigations presented so far on the Cr-alloyed PM steel under different sintering conditions and powder-based HIP provided the necessary background for full density consolidation of water atomised powder having normal oxygen levels for such powder [Paper IV]. This study presents the consolidation of water atomised powder through means of CIP. Figure 21 (a, b) presents the compressibility curve for both iron and Cr-alloyed powder; for these two variants the maximum green densities of around 7.55 g/cm^3 and 7.45 g/cm^3 were reached, respectively. The presence of lubricant affects the compressibility, whereas for the powder with and without graphite the densification behaviour was similar and the pressures beyond 600 MPa ensured reaching such high density levels.

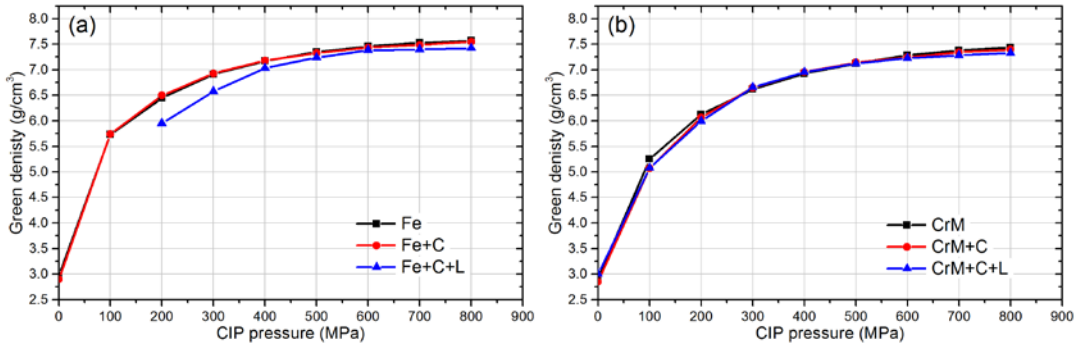

Figure 21: CIP compressibility curves of iron (a) and pre-alloyed with Cr (b) powder.

Sintering at 1120 °C gave similar density levels after CIP and did not provide any surface pore closure. Sintering at 1250 °C, however, enhances the sintered density to 7.60 g/cm^3 and 7.50 g/cm^3 for the iron and Cr-alloyed material, respectively. These values represent about 96% of the theoretical densities in the two cases. The open pores are transformed into closed pores, which become rounded and isolated as confirmed by the He-pycnometer measurements and microstructure analysis. However, the complete pore transition occurs only in the presence of graphite for Cr-alloyed PM steel, which indicates the significant role of carbon in reducing the oxides and assisting in forming better inter-particle necks. The minimum CIP pressure necessary for reaching pore closure after sintering at 1250 °C is about 500 MPa for Fe and 600 MPa for Cr-alloyed steel [Paper IV]. Figure 22 shows the optical micrograph of the Fe and CrM compacts with 0.4C after HIP, showing fully dense microstructures. The measured hardness values were very similar to the hardness values of fully dense wrought materials obtained from JMatPro simulations for the similar composition and cooling rate.

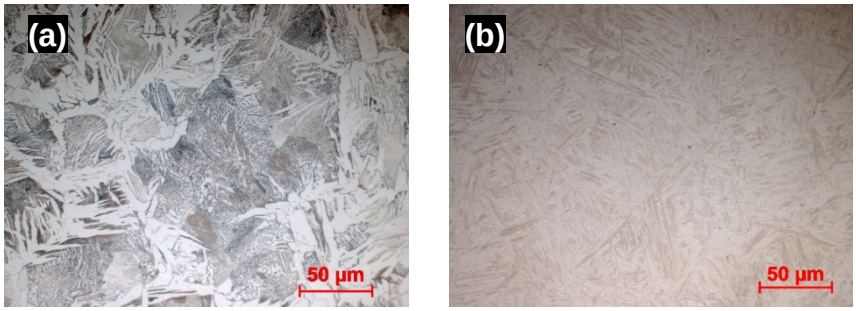

Figure 22: Optical micrograph of Fe+C (a) and CrM+C (b) after capsule-free HIP.

6.4.2 **Liquid phase sintering with boron-containing master alloy (Papers V & VI)**

The scope of this study was to evaluate the role of Ni-Mn-B master alloy addition on the densification behaviour of PM steel. The liquid phase generation was assessed using DSC and related to the resulting microstructure and mechanical properties of the compacts from dilatometry sintering. Formation of the liquid phase is found to occur in two stages involving the master alloy melting at around 1100 °C and eutectic reaction at around 1150 °C. The densification mechanism is hence a result of the liquid phase formation at different stages, as seen from the optical micrographs of the samples in Figure 23. The master alloy (MA) particle structure in Figure 23 (a) indicates partial melting of the MA particle. Once the master alloy is melted, the melt penetrates along the particle and grain boundaries causing rapid shrinkage through the initial particle rearrangement.

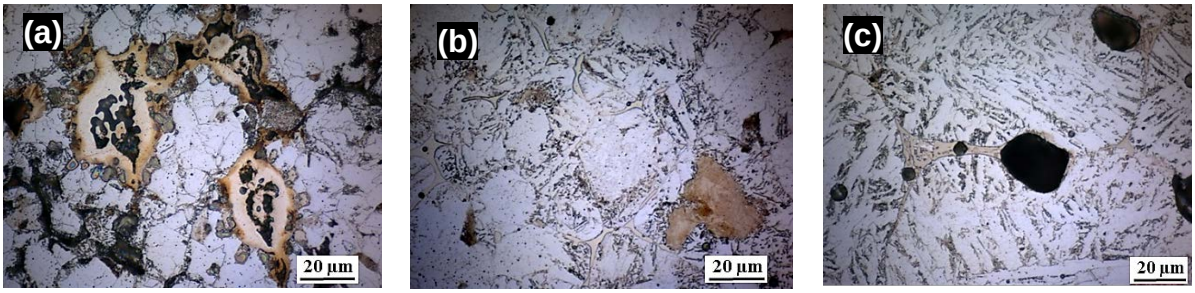

Figure 23: Optical micrographs of Fe-Mo+1.5MA+C after different sintering temperatures: 1000 °C-1 min (a), 1100 °C-1 min (b), and 1240 °C-30 min (c).

Once eutectic reaction then begins, the secondary liquid formation occurs and the final precipitation takes place, having the typical eutectic structure after sintering at 1240 °C, see Figure 23 (c). This is the characteristic behaviour observed for all the six powder mixes mentioned in Paper V. The effect of alloying content on the densification behaviour is shown in Figure 24. It is clear from the calculations presented in Paper V that the liquid phase content increases with higher master alloying content.

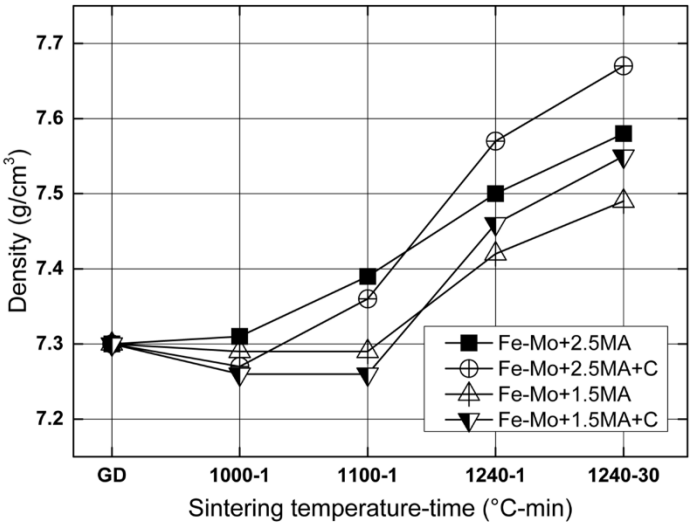

Figure 24: Density plot for Fe-Mo mixes with varying master alloy after interrupted sintering trails [Paper V].

Alloying elements, such as Mo and C, have a significant impact on densification behaviour and the properties. Both elements contribute to the higher liquid volume fraction and hence the increased density levels, see Figure 24. The presence of Mo plays a vital part in the liquid phase formation and is an essential element to be accounted for when adding B to realise improved mechanical properties. The results for mix with 2.5 wt.% of master alloy addition, however, showed embrittlement of sintered material, owing to the formation of continuous boride networks along the grain and particle boundaries, with such networks becoming more severe with increased amount of added carbon [93]. By decreasing master alloy content to 1.5 wt.% in the samples, however, the sintered material exhibited excellent ductility and impact energy beyond 100 J, which is similar to the Fe-0.1B variant [131]. The results indicated that the master alloy addition effectively enhanced the densification behaviour. The behaviour during sintering, along with the liquid phase generation, microstructural characteristics and mechanical testing revealed that the optimised master alloy addition by reducing it from 2.5 to 1.5 wt.% was necessary for better performance.

6.4.2.1 Surface densification

Sintering with the addition of 1.5 and 2.5 wt.% of Ni-Mn-B master alloy enabled reaching relative density levels of beyond 95% and displayed a surface densification phenomenon. Furthermore, the formation of such pore free surface layer is prominent especially when compacts are sintered either in hydrogen or hydrogen-containing atmospheres [25]. This gives the possibility to perform capsule free HIP to reach full densification. Figure 25 (a) and (b) shows the microstructure after sintering and capsule-free HIP, resulting in densification of up to 96% and 100%, respectively.

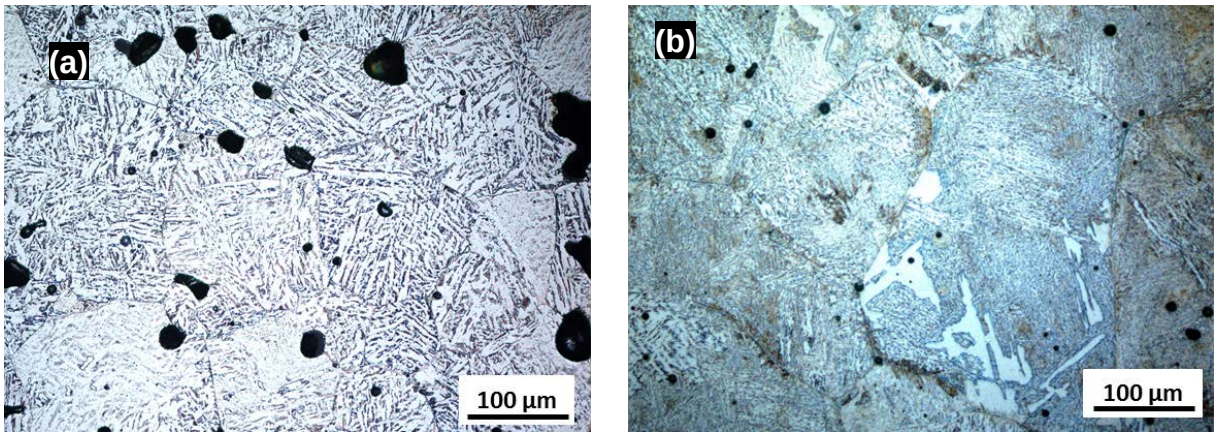

Figure 25: Optical micrograph of Fe-Mo+1.5MA+C specimens after sintering (a) and after HIP (b).

6.4.3 **Double pressing-double sintering approach**

The scope of this study was to evaluate the limits of double pressing and double sintering in the case of optimised powder pre-alloyed with Mo. Characterisation at different stages of the process was then performed as part of this thesis study to evaluate the effect of powder size fraction and the geometry of the specimens on the densification after final sintering and HIP.

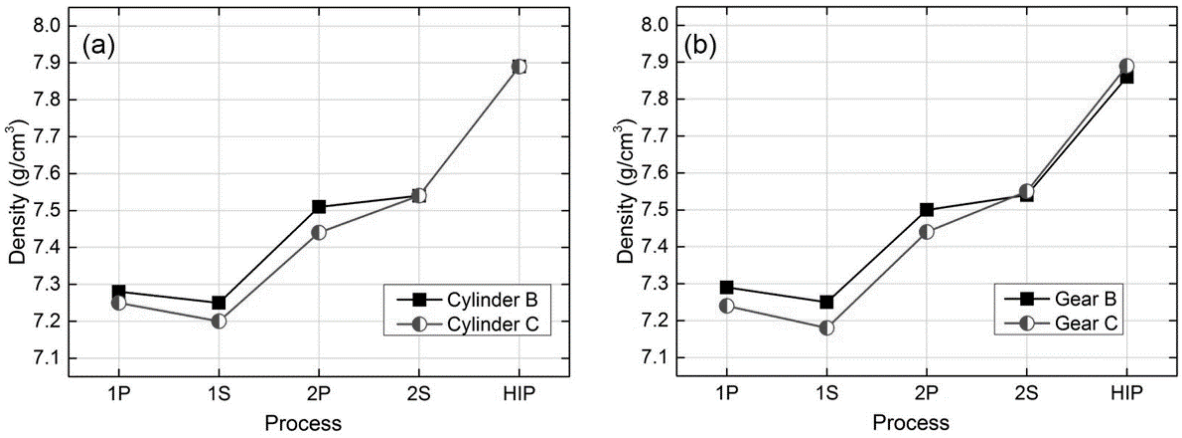

Figure 26: Density levels at different process stage for the Cylindrical (a) and Gear (b) specimens [Paper VII].

The results show that the double pressing-double sintering is sufficient for surface pore closure after sintering at 1300 °C for cylinders (B & C) and further HIP to full density, see Figure 26 (a). However, in the case of gear specimens, the lower densities were recorded, see Figure 26 (b). Both the cylindrical and gear specimens after DPDS reached a relative density of about 95%. When it comes to the samples made from standard and fine (< 63 µm) powder, the fine powder resulted in enhanced densification after second sintering owing to the size effect. For the simple cylindrical geometry, both the standard and fine powder samples resulted in full densification after capsule free HIP reaching ~7.89 g/cm^3.

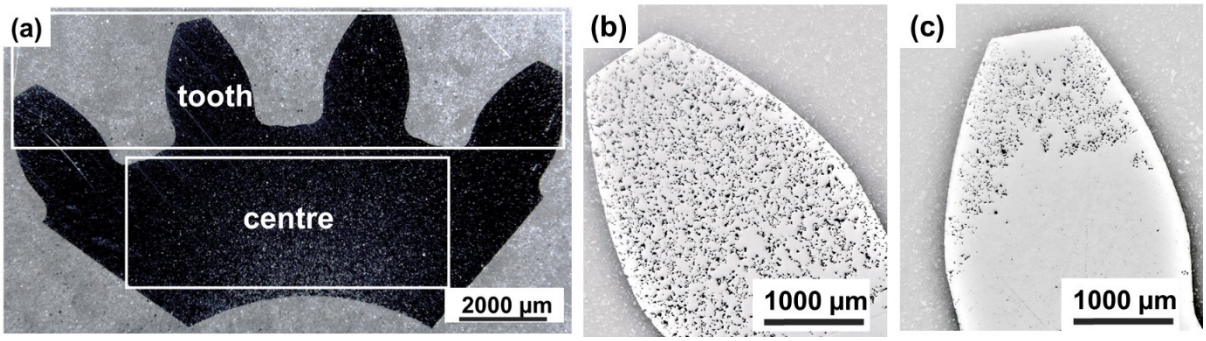

Figure 27: Micrographs of the gear cross section showing the analysed tooth and the centre region for the gear samples (a), tooth region of the samples after HIP sectioned at the neutral zone, Gear B (b) and Gear C (c) [Paper VII].

6.4.3.1 Neutral zone

For gear samples, it is evident that the neutral zone problem persists even after HIP processing. This phenomenon arises from the first pressing step where the density gradient or variation

within the compact arises due to the pressure gradient during compaction along the component height at the tool/powder compact interface. This, in fact, causes low-density levels in the middle region in the component surface, which persists even after HIP. This region is associated with the open pores on the surface and after HIP it will remain as the unclosed region as in Figure 27 (b & c). This is more evident in the case of coarse powder in gear specimens. A similar densification behaviour is also predicted by FEM simulations after pressing [132]. Even though the porosity values of the fine powder samples after first pressing and sintering are slightly higher, the average pore size is somewhat smaller than that for the standard powder samples [132]. This promotes better densification after second sintering and HIP. Considering the geometrical aspects, smaller gear tooth geometry will result in a neutral zone due to the incomplete powder filling, and this problem can be eliminated for larger gear geometry as shown in simulations observed from the powder pressing simulations [133], [134]. From this study it can be inferred that for complex geometries, like gears, having fine powder size fraction and sintering at high temperature is beneficial. This allows to have a pore closure on the surface which can be HIP-processed further without any capsule to full density.

7 CONCLUSIONS

7.1 Studies of PM steel pre-alloyed with Cr

7.1.1 Effect of sintering conditions on mechanical properties

The effect of the sintering parameters such as sintering temperature and process atmosphere have been analysed with resulting conclusions as follows.

- High sintering temperatures (>1200 °C) are needed for increasing the mechanical properties as well as to assure effective reduction of the surface bound oxygen.
- The influence of different vacuum levels on sintering is negligible when sintering at high temperatures.
- High density samples can be sintered with a good mechanical properties in vacuum or reducing gaseous atmosphere at high sintering temperatures of 1250 °C.

7.1.2 Effect of density on mechanical properties

- Increasing the density increases the properties following general relationship $P = P_0\left(\rho/\rho_0\right)^m$ as the strength of the material is determined by the increased load bearing sections.
- Powder-based HIP enables full densification and allows for reaching properties equivalent to that of wrought material.

7.1.3 Oxide reduction during sintering and HIP

Analysis of fracture surface after sintering indicates oxide transformation through different stages of sintering has been addressed with results as follows.

- Reduction of surface iron oxide layer by hydrogen at lower temperatures of around 450 to550 °C and by carbon at higher temperature (>800 °C) both play important role in the sintering of Cr-alloyed PM steel.
- Higher oxygen content in the water atomised powder results in higher content of the oxide phases in the powder-based directly HIP-processed components.
- The surface chemistry of the powder in terms of initial oxide thickness and potential transformation to stable oxide phases is significant for the final distribution of oxide particles at prior particle boundaries in the directly HIP-processed material and hence its resulting properties.

7.2 Full density consolidation processes

7.2.1 Cold isostatic pressing

- Consolidation of water atomised powder through CIP allows for reaching 95% relative density levels involving pressing without any lubricant addition.
- Sintering at high temperature in presence of carbon is essential to enable surface pore closure.
- Capsule-free HIP allows for full densification and the obtained properties are equivalent to those of the wrought material.
- It is demonstrated that the CIP→sinter→HIP is a potential processing route for full density consolidation starting from water atomised powder.

7.2.2 **Role of boron-containing master alloy**

The liquid phase sintering using recently developed boron-containing master alloy enabled following results.

- Enhanced densification of above 95% of the theoretical density after sintering is shown.
- The molybdenum and carbon means significant impact on the densification and final properties.
- Microstructural embrittlement occurs when master alloy addition is up to 2.5 wt.%.
- Carbon addition may also result in significant embrittlement of the final components.
- Optimised boron content for improved properties is around 0.12 wt.% (1.5 wt.% master alloy addition).
- Utilisation of the master alloy provides surface densification that allows subsequent HIP without any capsule to reach full density.

7.2.3 **Effect of double pressing-double sintering**

The double pressing-double sintering of standard and fine powders of iron pre-alloyed with 1.5 wt.% gave the following conclusions .

- High enough density to close the surface pores allows subsequent HIP without capsule.
- The result is near full density and hence this approach could be potential route for making fully dense PM parts.
- Still, the neutral zone problems associated with the pressing operation need to be addressed and tuned for successful final densification of parts in all locations by means of final capsule-free HIP.

8 SUGGESTIONS FOR FUTURE WORK

Though the emphasis in this thesis study has mainly been towards the densification aspects of the PM steel, some critical aspects were observed when it comes to the successfully achieving full densification.

8.1 Cold isostatic pressing and sintering

- In terms of CIP trails in case of water atomised powder, trails should be performed on the powder with lower amount of oxygen to reduce the overall impact of the oxygen content.
- The role of oxides and its influence on the mechanical properties are needed to be further evaluated, especially with respect to the fatigue properties.
- Economic feasibility of the approach has to be further developed.
- The CIP mould design and manufacturing should be optimised in order to realise near net shaping possibilities.

8.2 Hot isostatic pressing

- The effect of the oxygen content of water atomised powder and HIP parameters should be studied.
- The optimisation of HIP parameters such as temperature and pressure need to be developed for this type of material.
- The interaction and the influence of the argon atmosphere used in the HIP should be evaluated, considering the HIP being performed without any capsules.
- The possibility to integrate vacuum sintering, HIP and post heat treatment as a single process should be evaluated.

9 ACKNOWLEDGEMENTS

- I want to express my gratitude and thanks to my supervisors Prof. Lars Nyborg and Prof. Eduard Hryha for the opportunity and the freedom they gave me in the pursuit of powder metallurgy.
- All the support from Höganäs AB is greatly acknowledged, especially by Sigurd Berg, Dr. Ola Bergman, Dr. Michael Andersson and Dr. Dimitris Chasoglou, all from Höganäs AB, for providing the materials, additional experiments and technical support within the framework of several projects. Also, thanks are extended to Karin Ljung, Siv Olsson and Dmitri Riabov for helping me with the tests there.
- Magnus Ahlfors, Johannes Gårdstam and Dr. Anders Eklund from Quintus Technologies AB are greatly acknowledged for all the CIP, HIP trails, delightful discussions and collaboration.
- Dr. Hans Magnusson, Dr. Annika Strondl, and Dr. Irma Heikkilä from Swerim AB, are greatly acknowledged for all the collaboration within the framework of several projects.
- Dr. Karin Frisk currently at Höganäs AB is acknowledged for her support and help with calculations and also the collaborations with the projects in the beginning.
- Many thanks to Dr. Christer Åslund from Scandinavian Powdertech AB for all the inputs and the passionate discussions about metal powder.
- Thanks to Alireza Khodae from KTH and Prof. Arne Melander for their contribution as the co-authors and for the collaborations in the project.
- Thanks to all the other co-authors, academic and industrial partners, from CEIT Spain, Ruhr-Bochum Universität, AB Volvo, FJ Sintermetal AB, AGA AB, Mid Sweden University, within the several projects are greatly acknowledged. Support from Jernkontoret and Sweden's innovation agency VINNOVA in the following projects through the programmes Metalliska material and FFI are gratefully acknowledged, see list below.
    - Dnr: 2010-01619, High-performance sintered steels with high density and dimension control – next generation sintered steels (HIPERSINT)
    - Dnr: 2013-05594, Innovative powder based manufacturing of gear wheels with high performance (HIPGEAR)
    - Dnr: 2013-03299, Novel sintering strategy for the competitive manufacturing of the high-performance PM components (COMPRESINT)
    - Dnr: 2017-02531, New process technology for medium scale production of fully dense powder metallurgic materials and components (DENSE-PM)
    - Dnr: 2018-02371, Full Density PM-steel through New Processing Routes (DENSE)
    - Support from Swedish Foundation for Strategic Research (GMT14-045) is also gratefully acknowledged.
- All thanks are also extended to Dr. Yiming Yao, Dr. Eric Tam, Roger Sagdahl and Håkan Milqvist for the continuous help and solving any technical difficulties with the analysis and instruments.
- Then, I would like to thank Dr. Seshendra Karamchedu, Associate Professor Kumar Babu Surreddi, Dr. Henrik Karlsson for all the support, collaborations and the great discussions.

- Thanks to Dr. Ruslan Shvab, Alexander Leicht for all the support and collaboration, and Johan Wendel for the never-ending powder based discussions. Also, many thanks to Swathi and Adrianna for their presence in making the workplace more lively and exciting!
- My friends and colleagues at the current IMS and former MMT, are greatly acknowledged for all the collaboration, co-operation, and interactions through research, innebandy, badminton, and of course in food!!!.
- My sincere dedication to my late grandparents: Ammayi (அம்மாயி) and Thaatha (தாத்தா) for their blessings. And to my parents, family, and friends all around the world. Also, to my nephew and niece, who thinks, I am still going to school like them. Finally to Brindha….!

10 REFERENCES

[1] W. Schatt and K. P. Wieters, *Powder Metallurgy - Processing and Materials*. Shrewsbury: EPMA, 1997.

[2] "WORLDPM2018: Plenary sessions highlight continued growth for global Powder Metallurgy," *Powder Metallurgy Review*, pp. 79–85, 2018.

[3] R. M. German, *Powder Metallurgy of Iron and Steel*. Wiley-Interscience, 1998.

[4] J. R. Dale, "Powder Metallurgy -Intrinsically Sustainable," *International Journal of Powder Metallurgy*, 2011. [Online]. Available: https://www.mpif.org/IntroPM/PDFs/PM-Intrinsically-Sustainable.pdf.

[5] *Höganäs Handbook for Sintered Components 3: Design and Mechanical Properties*. Höganäs AB, 2004.

[6] R. M. German, *Powder Metallurgy & Particulate Materials Processing*. Princeton, NJ: Metal Powder Industries Federation, 2005.

[7] H. G. Rutz and F. G. Hanejko, "High density processing of high performance ferrous materials," *Adv. Powder Metall. Part. Mater.*, vol. 5, p. 117, 1994.

[8] F. Hanejko, "High Density via Single Pressing / Single Sintering," *Fenmo Yejin Jishu/Powder Metall. Technol.*, vol. 28, no. 1, pp. 73–76, 2010.

[9] "CES Edupack 2018." Granta Design Limited, Cambridge, UK, 2018.

[10] "European Powder Metallurgy Association (EPMA) - Powder Metallurgy Process." [Online]. Available: https://www.epma.com/powder-metallurgy-process. [Accessed: 26-Dec-2018].

[11] O. Grinder, "Plenary presentation: Key Areas for Development in PM Technology," in *Euro PM 2009*, 2009.

[12] "Powder Metallurgy Market Trends." [Online]. Available: http://www.strategyr.com/MarketResearch/Powder_Metallurgy_Market_Trends.asp. [Accessed: 22-Mar-2016].

[13] M. Ahlfors, "The Possibilities and Advantages with Heat Treatments in HIP," in *HIP14 Proceedings*, 2014.

[14] R. M. German, "Sintering With External Pressure," in *Sintering: from Empirical Observations to Scientific Principles*, Butterworth-Heinemann, 2014, pp. 305–354.

[15] M. Vattur Sundaram *et al.*, "Full densification in PM steels through liquid phase sintering and HIP approach," in *Euro PM 2018*, 2018.

[16] M. Vattur Sundaram, A. Khodaee, M. Andersson, L. Nyborg, and A. Melander, "Experimental and finite element simulation study of capsule-free hot isostatic pressing of sintered gears," *Int. J. Adv. Manuf. Technol.*, vol. 99, pp. 1725–1733, 2018.

[17] M. Vattur Sundaram, "Processing Methods for Reaching Full Density Powder Metallurgical Materials," Chalmers University of Technology, 2017.

[18] M. Hull, “Astaloy CrM: new generation powder from Höganäs,” *Powder Metall.*, vol. 41, no. 4, pp. 232–233, 1998.

[19] H. Karlsson, L. Nyborg, and O. Bergman, “Surface Interactions during Sintering of Water-atomised Pre-alloyed Steel Powder,” in *Euro PM2004*, 2004.

[20] O. Bergman, B. Lindqvist, and S. Bengtsson, “Influence of Sintering Parameters on the Mechanical Performance of PM Steels Pre-Alloyed with Chromium,” *Mater. Sci. Forum*, vol. 534–536, pp. 545–548, 2007.

[21] O. Bergman, “Influence of oxygen partial pressure in sintering atmosphere on properties of Cr–Mo prealloyed powder metallurgy steel,” *Powder Metall.*, vol. 50, no. 3, pp. 243–249, 2007.

[22] D. Chasoglou, E. Hryha, and L. Nyborg, “Effect of process parameters on surface oxides on chromium-alloyed steel powder during sintering,” *Mater. Chem. Phys.*, vol. 138, no. 1, pp. 405–415, Feb. 2013.

[23] S. Karamchedu, “Critical Aspects of Delubrication and Sintering of Chromium-alloyed Powder Metallurgy Steels,” Chalmers University of Technology, 2015.

[24] M. Sarasola, S. Sainz, and F. Castro, “Liquid Phase Sinterng of PM Steels Through Boron-Containing Master Alloy Additions,” in *Euro PM 2005*, 2005, vol. 1, pp. 349–356.

[25] A. Veiga, “Development of high performance nickel or boron PM steels respectively obtained after solid state and liquid phase sintering,” University of Navarra, San Sebastian, Spain, 2015.

[26] A. Flodin, M. Andersson, and A. Miedzinski, “Full density powder metal components through Hot Isostatic Pressing,” *Met. Powder Rep.*, pp. 2–5, 2016.

[27] R. M. German, *Powder Metallurgy and Particulate Materials Processing: The Processes, Materials, Products, Properties and Applications*. Metal Powder Industries Federation, 2005.

[28] J. R. Dale, “Powder metallurgy-intrinsically sustainable,” *Int. J. Powder Metall. (Princeton, New Jersey)*, vol. 47, no. 1, pp. 27–31, 2011.

[29] V. Kruzhanov and V. Arnhold, “Energy consumption in powder metallurgical manufacturing,” *Powder Metall.*, vol. 55, no. 1, pp. 14–21, 2012.

[30] C. Åslund and C. Quichaud, “Metallic powder for producing pieces by compression and sintering, and a process for obtaining this powder-US Patent,” 5460641, 1995.

[31] “Production of Sintered Components,” in *Höganäs Handbook 2*, Höganäs AB, 2004.

[32] W. Brian James, “High performance ferrous PM materials for automotive applications,” *Met. Powder Rep.*, vol. 46, no. 9, pp. 26–32, Sep. 1991.

[33] U. Engström, C. Lindberg, and J. Tengzelius, “Powders and processes for high performance PM steels,” *Powder Metall.*, vol. 35, no. 1, pp. 67–73, 1992.

[34] C. Recknagel, A. Marquardt, I. Langer, S. Müller, and B. Kieback, “Higher Densities

of PM-Steels by Warm Secondary Compaction and Sizing," *Proc. EURO PM 2011*, 2011.

[35] H. Karlsson, "Role of surface oxides in sintering of chromium-alloyed steel powder," Chalmers University of Technology, 2005.

[36] D. Chasoglou, "Surface Chemical Characteristics of Chromium-alloyed Steel Powder and the Role of Process Parameters during Sintering," Chalmers University of Technology, 2012.

[37] O. Bergman, "Key Aspects of Sintering Powder Metallurgy Steel Prealloyed with Chromium and Manganese," Chalmers University of Technology, 2011.

[38] W. B. James, "What is Sinter-Hardening?," in *International Conference on Powder Metallurgy & Particlulate Materials PM2TEC*, 1998, vol. 98, pp. 55–60.

[39] K. B. Surreddi, M. Vattur Sundaram, E. Hryha, H. Karlsson, M. Andersson, and L. Nyborg, "Low Temperature Creep Behavior of PM Components Under Static Load Conditions," in *Euro PM 2013, Sweden*, 2013, vol. 3, pp. 349–354.

[40] M. Vattur Sundaram *et al.*, "Investigation of Low Temperature Creep Behaviour of PM Steels," *Powder Metall. Prog.*, vol. 14, no. 2, pp. 67–72, 2014.

[41] P. Skoglund, M. Kejzelman, and I. Hauer, "High Density PM Components by High Velocity Compaction," in *Proc of 2002 World Congress on Powder Metallurgy*, 2002, vol. 4, pp. 85–95.

[42] F. Hanejko, "Warm Compaction and Warm Die Compaction," in *Powder Metallurgy*, vol. 7, P. Samal and J. Newkirk, Eds. ASM International, 2015, pp. 322–325.

[43] S. Lampman, "Compressibility and Compactibility of Metal Powders," in *Powder Metallurgy*, vol. 7, P. Samal and J. Newkirk, Eds. ASM International, 2015, pp. 171–178.

[44] U. Engström, B. Johansson, H. Rutz, F. Hanejko, and S. Luk, "High Density PM Materials for Future Applications," in *PA94*, 1994, vol. 1, pp. 57–64.

[45] W. B. James and K. S. Narasimhan, "Warm Compaction and Warm-Die Compaction of Ferrous PM Materials," *Trans. PMAI*, vol. 40, no. 1, pp. 15–22, 2014.

[46] C. Åslund and A. Eklund, "Preform CIP for fully dense PM parts," in *PowderMet 2012*, 2012, pp. 3126–3132.

[47] P. Skoglund, "High density PM parts by high velocity compaction," *Powder Metall.*, vol. 44, no. 3, p. 199, 2001.

[48] P. Jonsén, H. Å. Häggblad, L. Troive, J. Furuberg, S. Allroth, and P. Skoglund, "Green Body Behaviour of High Velocity Pressed Metal Powder," *Mater. Sci. Forum*, vol. 534–536, pp. 289–292, 2007.

[49] H. A. Kuhn, "Powder Hot Pressing and Forging," in *Powder Metallurgy*, vol. 7, P. Samal and J. Newkirk, Eds. ASM International, 2015, pp. 271–276.

[50] R. Tandon and J. Johnson, "Liquid Phase Sintering," in *Powder Metallurgy*, vol. 7, P.

Samal and J. Newkirk, Eds. ASM International, 1998, pp. 565–573.

[51] R. M. German, *Sintering Theory and Practice*. New York: John Wiley & Sons, Inc., 1996.

[52] R. M. German, *Liquid Phase Sintering*. Springer Science & Business Media, 1985.

[53] R. M. German, P. Suri, and S. J. Park, "Review: Liquid phase sintering," *J. Mater. Sci.*, vol. 44, no. 1, pp. 1–39, 2009.

[54] G. Zapf, G. Hoffmann, and K. Dalal, "Effect of additional alloying elements on the properties of sintered manganese steels," *Powder Metall.*, vol. 18, no. 35, pp. 214–236, Mar. 1975.

[55] A. Veiga and F. Castro, "Master Alloys for High Strength PM Steels," *World PM2012 Proc.*, no. 2, 2012.

[56] F. Castro, S. Sainz, A. Veiga, and P. Ortiz, "The Master Alloy Concept and its Consequences," in *Advances in Powder Metallurgy and Particulate Materials - 2012*, 2012.

[57] A. Veiga, C. Bilbao, S. Sainz, and F. Castro, "Controlled Shrinkage of Low Alloyed PM Steels During LPS," in *PowderMet2015*, 2015.

[58] M. N. Rahaman, "Sintering Theory and Fundamentals," in *Powder Metallurgy*, vol. 7, P. Samal and J. Newkirk, Eds. ASM International, 2015, pp. 205–236.

[59] K. E. Meiners and J. . McCall, "Recent Developments in HIP Technology," *Met. Powder Rep.*, 1981.

[60] D. Richter, G. Haour, and D. Richon, "Hot isostatic pressing (HIP)," *Mater. Des.*, vol. 6, no. 6, pp. 303–305, Dec. 1985.

[61] R. Ekbom, "Hot isostatic pressing/powder metallurgy in gas and steam turbines," *Mater. Des.*, vol. 11, no. 1, pp. 37–42, 1990.

[62] A. C. Nyce, "Containerless HIPing of PM Parts: Technology, Economics and Equipment Productivity," *Met. Powder Rep.*, vol. 38, no. 7, pp. 387–392, 1983.

[63] H. Magnusson *et al.*, "Reaching full density of 100Cr6 PM steel by capsule free hot isostatic pressing of high-velocity compacted material," in *World Powder Metallurgy 2016 Congress and Exhibition, World PM 2016; Hamburg; Germany; 9 October 2016 through 13 October 2016*, 2016.

[64] S. Das, M. Wholert, J. J.Beaman, and D. L.Bourell, "Producing metal parts with selective laser sintering/hot isostatic pressing," *JOM*, vol. 51, pp. 2–2, 1999.

[65] A. Eklund and M. Ahlfors, "Heat treatment of PM parts by Hot Isostatic Pressing," *Met. Powder Rep.*, vol. 73, no. 3, pp. 163–169, 2018.

[66] R. D. S. J. Matthew M. Diem, Stephen J. Mashl, "A Combination HIP + Heat Treat Process," *Heat Treating Progress*. 2003.

[67] A. Weddeling and W. Theisen, "Energy and time saving processing: A combination of hot isostatic pressing and heat treatment," *Met. Powder Rep.*, vol. 72, no. 5, pp. 345–

348, 2017.

[68] M. Andersson *et al.*, “Manufacturing Full Density Powder Metallurgy Gears through HIP:ing,” *Met. Powder Rep.*, 2019.

[69] A. Leicht *et al.*, “As-HIP Microstructure of EBM Fabricated Shell Components,” in *World PM 2016*, 2016.

[70] E. Hryha *et al.*, “Hot Isostatic Pressing of the Water Atomised Steel Powder: Possibilities and Challenges,” in *World PM 2018*, 2018.

[71] S. Tammas-Williams, H. Zhao, F. Léonard, F. Derguti, I. Todd, and P. B. Prangnell, “XCT Analysis of the Influence of Melt Strategies on Defect Population in Ti-6Al-4V Components Manufactured by Selective Electron Beam Melting,” *Mater. Charact.*, vol. 102, pp. 47–61, Feb. 2015.

[72] W. Tillmann, C. Schaak, J. Nellesen, M. Schaper, M. E. Aydinöz, and K. P. Hoyer, “Hot isostatic pressing of IN718 components manufactured by selective laser melting,” *Addit. Manuf.*, vol. 13, pp. 93–102, 2017.

[73] A. Nicolas *et al.*, “Analyzing the effects of powder and post-processing on porosity and properties of electron beam melted Ti-6Al-4V,” *Mater. Res. Lett.*, vol. 5, no. 7, pp. 516–525, 2017.

[74] H. Magnusson, J. Komenda, P. Mellin, M. Vattur Sundaram, and L. Nyborg, “Internal Report - KIMAB,” 2018.

[75] A. Liersch, H. Danninger, and R. Ratzi, “The Role of Admixed Hexagonal Boron Nitride in Sintered Steels 2 . Effect on Sliding Wear and Machinability,” *Powder Metall. Prog.*, vol. 7, no. 2, p. 2007, 2007.

[76] R. M. German, *Powder Metallurgy & Particulate Materials Processing*. Metal Powder Industries Federation, 2005.

[77] *Höganäs Handbook for Sintered Components 1: Materials and Powder Properties*. Höganäs AB, 2004.

[78] R. M. German, *Particle packing characteristics*. Princeton, NJ: Metal Powder Industries Federation, 1989.

[79] A. Bose, “Introduction to Metal Powder Injection Molding,” in *Powder Metallurgy*, vol. 7, P. Samal and J. Newkirk, Eds. ASM International, 2015, pp. 823–847.

[80] J. Klein, “Preliminary investigation of liquid phase sintering in ferrous systems,” California Univ., Berkeley (USA). Lawrence Berkeley Lab., 1975.

[81] D. S. Madan and R. M. German, “Enhanced Sintering for Ferrous Components,” in *Modern Developments in Powder Metallurgy.*, 1984, vol. 15, pp. 441–454.

[82] K. S. Narasimhan and F. J. Semel, “Sintering of Powder Premixes-A Brief Overview,” *Adv. POWDER Metall. Part. Mater.*, vol. 1, p. 5, 2007.

[83] R. M. German, K. S. Hwang, and D. S. Madan, “Analysis of Fe-Mo-B sintered alloys,” *Powder Metall. Int.*, vol. 19, no. 2, pp. 15–18, 1987.

[84] M. Selecká, A. Šalak, and H. Danninger, “The effect of boron liquid phase sintering on properties of Ni-, Mo- and Cr-alloyed structural steels,” *J. Mater. Process. Technol.*, vol. 143, pp. 910–915, 2003.

[85] L. Lozada and F. Castro, “Controlled densification of boron-containing stainless steels,” in *Advances in Powder Metallurgy and Particulate Materials*, 2011, pp. 778–788.

[86] J. C. Rodriguez, L. Lozada, C. Tojal, T. Gómez-Acebo, and F. Castro, “Thermodynamic Aspects of Liquid Phase Sintering B-Containing P/M Stainless Steels,” *Solid State Phenom.*, vol. 172–174, pp. 1164–1170, 2011.

[87] R. M. German, *Sintering Theory and Practice*. New York: John Wiley & Sons, 1996.

[88] D. Krecar, V. Vassileva, H. Danninger, and H. Hutter, “Characterization of the distribution of the sintering activator boron in powder metallurgical steels with SIMS.,” *Anal. Bioanal. Chem.*, vol. 379, no. 4, pp. 605–9, Jun. 2004.

[89] M. Sarasola, T. Gómez-Acebo, and F. Castro, “Liquid generation during sintering of Fe–3.5%Mo powder compacts with elemental boron additions,” *Acta Mater.*, vol. 52, no. 15, pp. 4615–4622, Sep. 2004.

[90] J. Karwan-Baczewska and M. Rosso, “THE EFFECT OF BORON ON THE PROPERTIES OF Fe-Mo PM SINTERED ALLOYS,” *Powder Metall. Prog.*, vol. 6, no. 1, pp. 11–19, 2006.

[91] W. Wang, S. Zhang, and X. He, “Diffusion of boron in alloys,” *Acta Metall. Mater.*, vol. 43, no. 4, pp. 1693–1699, Apr. 1995.

[92] M. Marucci, A. Lawley, R. Causton, and S. Saritas, “Effect of Small Additions of Boron on the Mechanical Properties and Hardenability of Sintered PM steels,” *Proc. Powder Metall. Congr. Exhib. Orlando, Florida, USA*, 2002.

[93] C. Gierl-mayer, J. Zbiral, and H. Danninger, “Enhanced Sintering of PM Steels by Addition of Fe-Ni-B Masteralloy,” in *Euro PM2014*, 2014, pp. 1–6.

[94] M.-W. Wu and W.-Z. Cai, “Phase identification in boron-containing powder metallurgy steel using EBSD in combination with EPMA,” *Mater. Charact.*, vol. 113, pp. 90–97, Mar. 2016.

[95] M.-W. Wu and W.-Z. Cai, “The Promotion of Liquid Phase Sintering of Boron-Containing Powder Metallurgy Steels by Adding Nickel,” in *MATEC Web of Conferences*, 2015, vol. 27, p. 01012.

[96] M.-W. Wu, “The Influences of Carbon and Molybdenum on the Progress of Liquid Phase Sintering and the Microstructure of Boron-Containing Powder Metallurgy Steel,” *Metall. Mater. Trans. A*, vol. 46, no. 1, pp. 467–475, Oct. 2014.

[97] A. K. Mashkov, V. I. Gurdin, and E. P. Polyakov, “A boron-containing material for the infiltration of iron compacts,” *Sov. Powder Metall. Met. Ceram.*, vol. 18, no. 5, pp. 344–346, 1979.

[98] P. Beiss, “Iron and steel: manufacturing route, chap 5, structural mass production,” in

Landolt-Börnstein—Group VIII Advanced Materials and Technologies, 2003, pp. 5–20.

[99] G. F. Bocchini, "The influence of porosity on the characteristics of sintered materials," *Int. J. powder Metall.*, vol. 22, no. 3, pp. 185–202, 1986.

[100] H. Danninger, G. Jangg, P. Beiss, and R. Stickler, "Microstructure and mechanical properties of sintered iron. II: Experimental study," *PMI. Powder Metall. Int.*, vol. 25, no. 5, pp. 219–223, 1993.

[101] I. Hauer, M. Larsson, and U. Engström, "Properties of high-strength PM materials obtained by different compaction methods in combination with high temperature sintering," *Adv. Powder Metall. Part. Mater.*, vol. 8, pp. 8–29, 2002.

[102] N. Chawla, J. J. Williams, X. Deng, C. Mcclimon, L. Hunter, and S. H. Lau, "Three-dimensional characterization ahd modeling of porosity in PM steels," *Int. J. Powder Metall. (Princeton, New Jersey)*, vol. 45, no. 2, pp. 19–27, 2009.

[103] X. Xu, W. Yi, and R. M. German, "Densification and strength evolution in solid-state sintering. Part I Experimental investigation," *J. Mater. Sci.*, vol. 37, no. 3, pp. 567–575, 2002.

[104] E. Dudrova and M. Kabátova, "A review of failure of sintered steels: fractography of static and dynamic crack nucleation, coalescence, growth and propagation," *Powder Metall.*, vol. 59, no. 2, pp. 148–167, 2016.

[105] E. Dudrová and M. Kabátová, "Fractography of Sintered Iron and Steels," *Powder Metall. Prog.*, vol. 8, no. 2, pp. 59–75, 2008.

[106] C. Menapace, a. Molinari, J. Kazior, and T. Pieczonka, "Surface self-densification in boron alloyed austenitic stainless steel and its effect on corrosion and impact resistance," *Powder Metall.*, vol. 50, no. 4, pp. 326–335, Dec. 2007.

[107] B. Dubrujeaud, M. Vardavoulias, and M. Jeandin, "The role of porosity in the dry sliding wear of a sintered ferrous alloy," *Wear*, vol. 174, no. 1–2, pp. 155–161, 1994.

[108] X. Li, "Efficiency and wear properties of spur gears made of powder metallurgy materials-PhD Thesis," KTH Royal Institute of Technology, 2016.

[109] T. Takashita, A. Kobayashi, and N. Nakamura, "Influence of Pore Size on Toughness of Fe-Mo-Cu-C Sintered and Carburized Components," *Euro PM2018*, 2018.

[110] L. Forden, S. Bengtsson, and M. Bergström, "High performance gears," in *Euro PM2004*, 2004.

[111] R. Haynes, "Effects of porosity on the tensile strengths of sintered irons," *Met. Powder Rep.*, vol. 46, no. 2, pp. 49–51, Feb. 1991.

[112] L. Fuentes-Pacheco and M. Campos, "Bonding evolution with sintering temperature in low alloyed steels with chromium," *Sci. Sinter.*, vol. 41, no. 2, pp. 161–173, 2009.

[113] P. Ortiz and F. Castro, "Thermodynamic and experimental study of role of sintering atmospheres and graphite additions on oxide reduction in Astaloy CrM powder compacts," *Powder Metall.*, vol. 47, no. 3, pp. 291–298, Sep. 2004.

[114] U. Engström, “Influence of sintering temperature on properties of low alloyed high strength PM materials,” in *Advances in Powder Metallurgy and Particulate Materials*, 2001, pp. 1418–1429.

[115] M. Dlapka, H. Danninger, C. Gierl, and B. Lindqvist, “Defining the pores in PM components,” *Met. Powder Rep.*, vol. 65, no. 2, pp. 30–33, Feb. 2010.

[116] E. Hryha and L. Nyborg, “Thermogravimetry study of the effectiveness of different reducing agents during sintering of Cr-prealloyed PM steels,” *J. Therm. Anal. Calorim.*, vol. 118, no. 2, pp. 825–834, Jul. 2014.

[117] M. Vattur Sundaram, S. Karamchedu, C. Gouhier, E. Hryha, and L. Nyborg, “Vacuum sintering studies on chromium alloyed PM steels,” in *World PM 2016*, 2016.

[118] D. Chasoglou, E. Hryha, M. Norell, and L. Nyborg, “Characterization of surface oxides on water-atomized steel powder by XPS/AES depth profiling and nano-scale lateral surface analysis,” *Appl. Surf. Sci.*, vol. 268, pp. 496–506, Mar. 2013.

[119] K. Hariramabadran Anantha, “Study of Total Oxygen Content and Oxide composition Formed During Water Atomization of Steel Powders due to Manganese Variation.” 2012.

[120] D. Chasoglou, E. Hryha, and L. Nyborg, “Surface interactions during sintering of chromium-alloyed PM steels in different atmospheres,” *Proc. WORLD PM 2010*, vol. 2, p. 3, 2010.

[121] E. Hryha and L. Nyborg, “Oxide Transformation in Cr-Mn-Prealloyed Sintered Steels: Thermodynamic and Kinetic Aspects,” *Metall. Mater. Trans. A*, vol. 45, no. 4, pp. 1736–1747, Sep. 2014.

[122] M. Vattur Sundaram, E. Hryha, and L. Nyborg, “XPS Analysis of Oxide Transformation During Sinteirng of Chromium Alloyed PM Steels,” *Powder Metall. Prog.*, vol. 14, no. 2, pp. 85–92, 2014.

[123] H. He *et al.*, “Effects of oxygen contents on sintering mechanism and sintering-neck growth behaviour of Fe–Cr powder,” *Powder Technol.*, vol. 329, pp. 12–18, 2018.

[124] A. Lind, J. Sundström, and A. Peacock, “The effect of reduced oxygen content powder on the impact toughness of 316 steel powder joined to 316 steel by low temperature HIP,” *Fusion Eng. Des.*, vol. 75, pp. 979–983, 2005.

[125] A. Angré and A. Strondl, “The effect of drastically lowered oxygen levels on impact strength for HIP’ed 316L material,” in *HIP14 Proceedings*, 2014, pp. 205–211.

[126] A. J. Cooper, N. I. Cooper, J. Dhers, and A. H. Sherry, “Effect of Oxygen Content Upon the Microstructural and Mechanical Properties of Type 316L Austenitic Stainless Steel Manufactured by Hot Isostatic Pressing,” *Metall. Mater. Trans. A*, vol. 47, no. 9, pp. 4467–4475, Sep. 2016.

[127] T. Berglund and F. Meurling, “Oxygen Content in PM HIP 625 and its Effect on Toughness,” in *Material Research Proceedings*, 2019, vol. 10, pp. 135–141.

[128] E. Hryha *et al.*, “Surface Oxide Transformation during HIP of Austenitic Fe-19Mn-

18Cr-C-N PM Steel," in *Proceedings of 11-th International Conference on Hot Isostatic Pressing*, 2014, pp. 180–193.

[129] A. J. Cooper, W. J. Brayshaw, and A. H. Sherry, "Tensile Fracture Behavior of 316L Austenitic Stainless Steel Manufactured by Hot Isostatic Pressing," *Metall. Mater. Trans. A*, vol. 49, no. 5, pp. 1579–1591, 2018.

[130] *Handbook of X-ray Photoelectron Spectroscopy*. Perkin-Elmer Corporation.

[131] V. Vassileva, H. Danninger, S. Strobl, and C. Gierl, "Atmosphere Effects on Sintering of Ferrous Powder Compacts Containing Boron," in *Euro PM2007*, 2007, vol. 1, no. 1, pp. 53–58.

[132] A. Khodaee *et al.*, "Innovative Powder Based Manufacturing of High Performance Gears," in *WORLD PM - PM Gears*, 2016, pp. 1–6.

[133] A. Khodaee and A. Melander, "Evaluation of effects of geometrical parameters on density distribution in compaction of PM gears," *AIP Conf. Proc.*, vol. 1896, no. 1, Oct. 2017.

[134] A. Khodaee and A. Melander, "Numerical and Experimental Analysis of the Gear Size Influence on Density Variations and Distortions during the Manufacturing of PM Gears with an Innovative Powder Processing Route Incorporating HIP," *J. Manuf. Mater. Process.*, vol. 2, no. 49, 2018.